Hydrogen Bonding in Perovskite Solar Cells

Liangyou Lin[1,], Timothy W. Jones[2], Terry Chien-Jen Yang[3,4], Xinyu Li[5], Congcong Wu[1], Zichen Xiao[1], Haijin Li[6], Jinhua Li[1], Jingwen Qian[1], Lin Lin[7], Javen Qinfeng Shi[5], Samuel D. Stranks[3,4], Gregory J. Wilson[2,*], and Xianbao Wang[1,*]*

[1]Key Laboratory for the Green Preparation and Application of Functional Materials Ministry of Education, School of Materials Science and Engineering, Hubei University Wuhan 430062, China

[2]CSIRO Energy Newcastle Energy Centre, 10 Murray Dwyer Circuit, Mayfield West, NSW 2304, Australia

[3]Department of Chemical Engineering and Biotechnology, University of Cambridge, Cambridge, UK

[4]Cavendish Laboratory, Department of Physics, University of Cambridge, Cambridge, UK

[5]Australian Institute for Machine Learning, The University of Adelaide, Adelaide, SA 5000, Australia

[6]Institute of Photovoltaics, Southwest Petroleum University, Chengdu 610500, China

[7]Biogen, 225 Binney Street, Cambridge, MA 02142, USA.

Correspondence: Lead Contact Liangyou_Lin@hubu.edu.cn (L.L); Gregory.Wilson@csiro.au (G.J.W); wxb@hubu.edu.cn (X.W);

Abstract

The efficiency of single-junction perovskite solar cells (PSCs) has reached 26.1% and greater attention is turning to improving their intrinsic and environmental stability. The optoelectronic properties of perovskites and interaction within a device depend not only on their component atoms but also neighboring atoms. It is necessary to further understand and explore the interaction between the functional material and device. Here, we summarize the hydrogen bonding in PSCs, including each functional layer and interface. Despite being a weak force, hydrogen bonding can greatly influence material properties. Effects on crystallization, stability, ion migration, phase transition etc., and strategies to precisely adjust hydrogen bonding for target properties are discussed. We observe that the research on hydrogen bonding in PSC is still controversial and poorly understood, thus it is often overlooked. With greater understanding, we anticipate researchers can further harness hydrogen bonding as a versatile tool to solve technical challenges in PSCs.

Key Word: hydrogen bonding, perovskite solar cell, stability, weak-interaction, high-performance

Introduction

The record power conversion efficiency (PCE) of single-junction halide perovskite solar cells (PSCs) has reached 26.1%, and recently 33.7% for a perovskite/Si tandem.[1] The rapid and impressive achievement makes halide perovskites the most promising candidate for the next generation of photovoltaic technology. With a PCE attractive enough for commercialization, attention is turning to improve the intrinsic and environmental stability of the PSC.[2,3,4] The optoelectronic properties such as absorption coefficient and charge carrier lifetime of perovskite materials and their interaction within a whole device depend not only on their component atoms but also influenced by neighbouring atoms.[5,6] We need to understand further and explore the interaction between the functional material and device to optimise the performance.

The inter/intramolecular chemical bonds and forces interaction spans from strong bonds, such as ionic, covalent and metallic bonds, to weak interactions, such as hydrogen bonds, van der Waals forces and halogen bonds.[7] The ionic bond is the electrostatic forces that exist between ions of opposite charge. The covalent bond is the sharing of an electron pair between two atoms. Metallic bonds are usually found in metals where each metal atom bonded to neighboring metal atoms and the bonding electrons are free to move throughout. The van der Waals force originates from the transient fluctuations in the electron density. This is a distance-dependent force.[5] These interactions play key roles in materials/devices, such as PSCs. Compared to the interactions outlined above, the influence of hydrogen bonding in devices is more complicated and controversial. Due to the greater difficulty of characterizing hydrogen bonds, understanding their influence on PSCs is lagging.

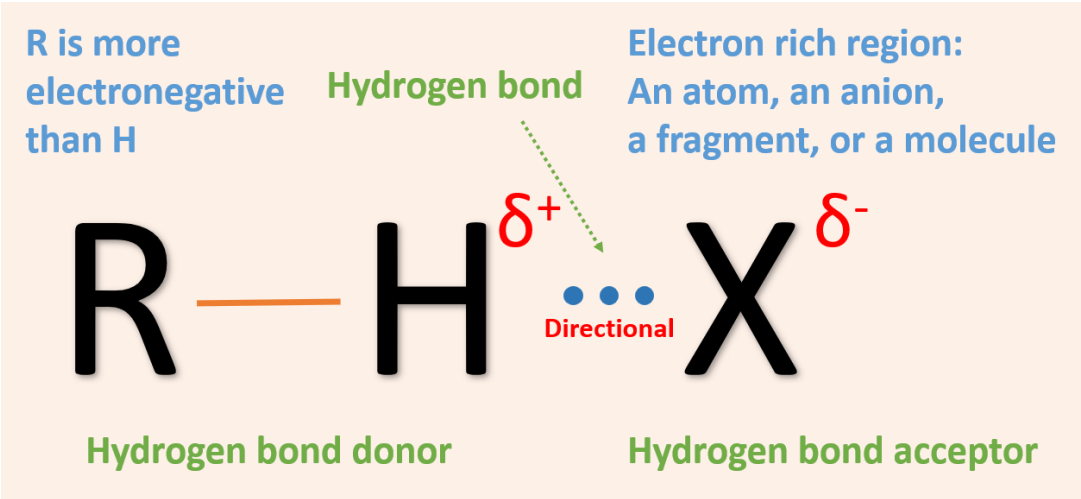

Figure 1. Schematic illustration of a hydrogen bond.

This review focuses on the weak interaction of hydrogen bonding within PSCs. Despite being a "weak" force, it can greatly influence material properties. For example, why does ice float on water? This is because hydrogen bonding forms a crystal structure that is of a lower density than the liquid form.[8] Water's natural hydrogen bonding network destabilizes its H-O···H bonds, resulting in easier bond cleavage and a narrow electrochemical window. Water's strong intermolecular hydrogen bonding network is partly responsible for its narrow 1.23 V electrochemical window. Interrupting this native H-bond network solutes or additives can expand the window beyond 3 V.[9,10] It is worth noting that hydrogen bonding is of great importance in biological systems where protein folding and the pairing of DNA bases as the most prominent examples.[7] The salt guanidinium chloride (GUACl) can be used by biologists to de-nature proteins, by disrupting their hydrogen bonding.[11] Now, the same GUA^+ is finding increased use in perovskite solar cells. More discussion about GUA^+ will be presented in a later section.

According to the modern definition made by International Union of Pure and Applied Chemistry, the hydrogen bond is an attractive interaction between a hydrogen atom from a molecule or a molecular fragment.[12] For most cases, it is enough to describe a hydrogen bond R-H···X shown in Figure 1, as an electrostatic attraction between the positive end of the bond dipole of R-H, and a center of negative charge on X.[13] The three dots denote the hydrogen bond. The R-H represents the hydrogen bond donor, the X represents the hydrogen bond acceptor, which can be an atom or an anion or a molecule.[12] The H atom is bonded to electronegative atoms such as N, O, and F. X is either an electronegative region or a region of electron excess. The main properties of hydrogen bonds are listed in Table 1. However, the definitions of weak and strong bonds may change from author to author.[7] Moreover, a hydrogen bond is also the most important directional intermolecular interaction. The tunable strength and directionality make hydrogen bonding an effective tool for adjusting the properties of materials and devices.[14,15] As a weaker force, researchers may often overlook the influence of hydrogen bonding. However, more researches have indicated the hydrogen bonding can work on both bulk and the interfaces between each functional layer which further affect the performance and stability of devices.[16,17]

Characterization of hydrogen bonding

Hydrogen bonding usually merges continuously with covalent/ionic bonds and van der Waals. Neither experimental nor computational methods can easily distinguish the individual contribution

Table 1. Main properties of hydrogen bonds.[7]

	Weak	Strong	Very strong
Electrostatics/ polarization	Moderate	Dominant	Significant
Quantum-mechanical contribution	Vanishing	Weak	Pronounced
Dissociation energy (-kcal/mol)	~1-4	~4-15	~15-40
Examples	C-H···O C-H···N	O-H···O=C N-H···O=C O-H···O-H	N-H···N F-H···F

to the bond energies. However, we can read the interaction via typical characterizations shown in Figure 2. Nuclear magnetic resonance (NMR) is the most common measurement to detect hydrogen bonding. This interaction is inferred by the change of the chemical shift.[18,19,20] Hydrogen bonding distorts the electron density cloud around the hydrogen nucleus, affecting the magnetic field. Thus the shielding effect of the hydrogen atom is changed and induces a change of chemical shift.[21] Han *et al*. observed that the resonance signals arising from the -OH protons are obviously broad, indicative of the OH···I hydrogen bonding interaction when adding poly(vinyl alcohol) into $FASnI_3$.[22] Vibrational spectroscopy is also a valuable tool for investigating hydrogen bonding since its formation changes bond oscillation strength. Fourier transform infrared spectroscopy (FTIR) is another convenient technique to detect hydrogen bonding by checking the typical chemical bond stretching vibration.[23] The shifted stretching peak are usually related to N-H, C=N, etc. chemical bonds from the organic cation in perovskite.[16] Raman spectroscopy is a powerful technique that is complementary with FTIR.[24] Tan *et al*. conducted Raman spectroscopic measurements to provide fingerprint information about the details of perovskite's organic–inorganic interactions by analysing the band shift. They also found for $MAPbX_3$ perovskite that an increase of the Cl content can strengthen the hydrogen bonding interaction, thus inducing a blueshift of the C–N stretching bands in Raman spectra.[24] X-ray photoelectron

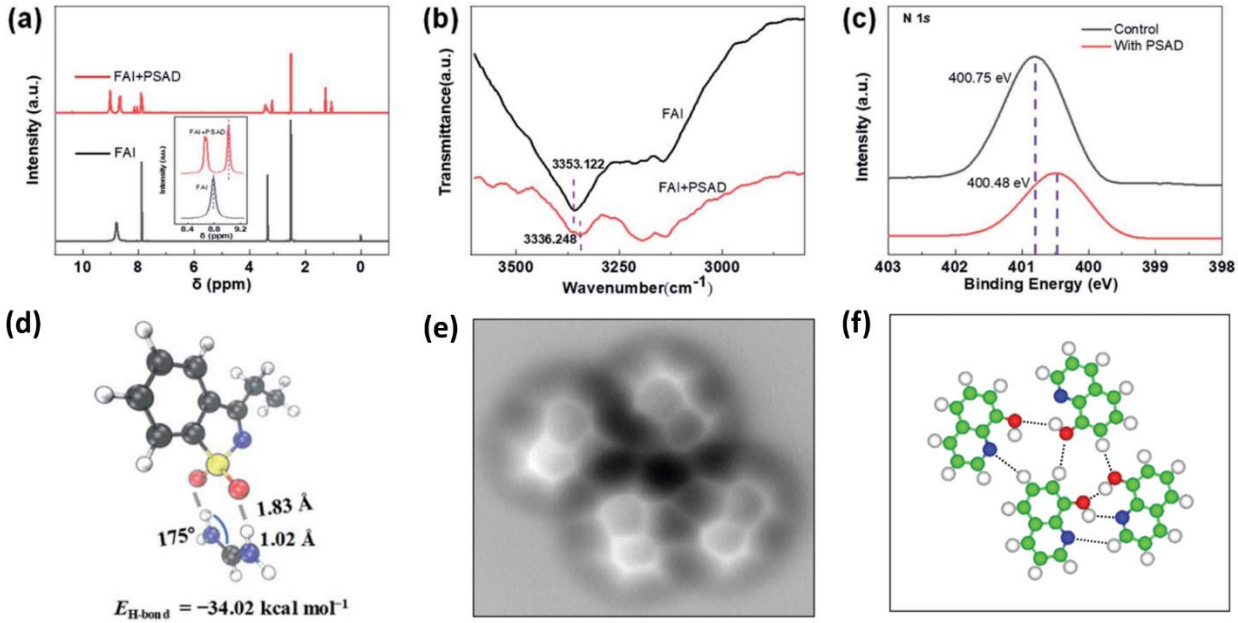

Figure 2. (a) ^{1}H NMR and (b) FTIR spectrum of formamidinium iodide films. (c) XPS spectra of perovskite films. (d) density functional theory (DFT) calculations of hydrogen bonds.[25] Copyright 2022, The Royal Society of Chemistry. (e) AFM images on Cu(111) and (f) the corresponding structure models.[26] Copyright 2013, American Association for the Advancement of Science.

spectroscopy (XPS) is usually conducted to check the binding energy of typical chemical state of elements. From the binding energy change, we can speculate the hydrogen bonding interaction to a certain extent.[25] However, XPS can only detect the interaction on the surface of perovskite materials/films. Site- and element-specific soft X-ray spectro-scopic measurement has been used to probe the electronic structure of perovskite. Odelius *et al*. found that femtosecond dynamics induced by core excitation strongly influence the measured X-ray emission and the resonant inelastic soft X-ray scattering of hybrid perovskite. The existing hydrogen bonding cause the electronic hybridization can be detected.[27] However, we need to avoid the beam damage when conducting this measurement. Qiu *et al*. use noncontact atomic force microscopy (NC-AFM) to realize a real-space visualization of the formation of hydrogen bonding. The atomically resolved molecular structures precisely determine the characteristics of hydrogen bonding networks. [26] The images are shown in Figure 2e and f.

Hydrogen bonds in perovskite materials

The formula ABX_3 (A= methylammonium, MA^+; formamidinium, FA^+; or cesium ion, Cs^+; B= lead ion, Pb^{2+}; or tin ion, Sn^{2+}; X= iodide ion, I^-; bromide ion, Br^-; or chloride ion, Cl^-) is the most commonly used three dimensional (3D) perovskite in PSCs.[28] The A and B cations coordinate with 12 and 6 X anions, respectively, forming a cuboctahedral and octahedral geometry, respectively.[29] The hydrogen bonding is usually formed between the organic cations (MA^+, FA^+) and the surrounding inorganic anions.[30] Since the electronic density of states originates from the inorganic PbX_3^- lattice, hydrogen-bonding between organic cations and the inorganic lattice can affect the properties of the perovskite semiconductor. The typical hydrogen bonding interaction in perovskite is between the ammonium group and iodide ion N-H···I.[31] Jang *et al*. demonstrated two distinct types (corresponding to the different tilt angle of the C-N bond) of the hydrogen bonding interaction in the tetragonal $MAPbI_3$ on symmetry argument using DFT calculations, as shown in Figure 3.[32] The calculated hydrogen bonding energy in typical 3D perovskites listed in Table 2.

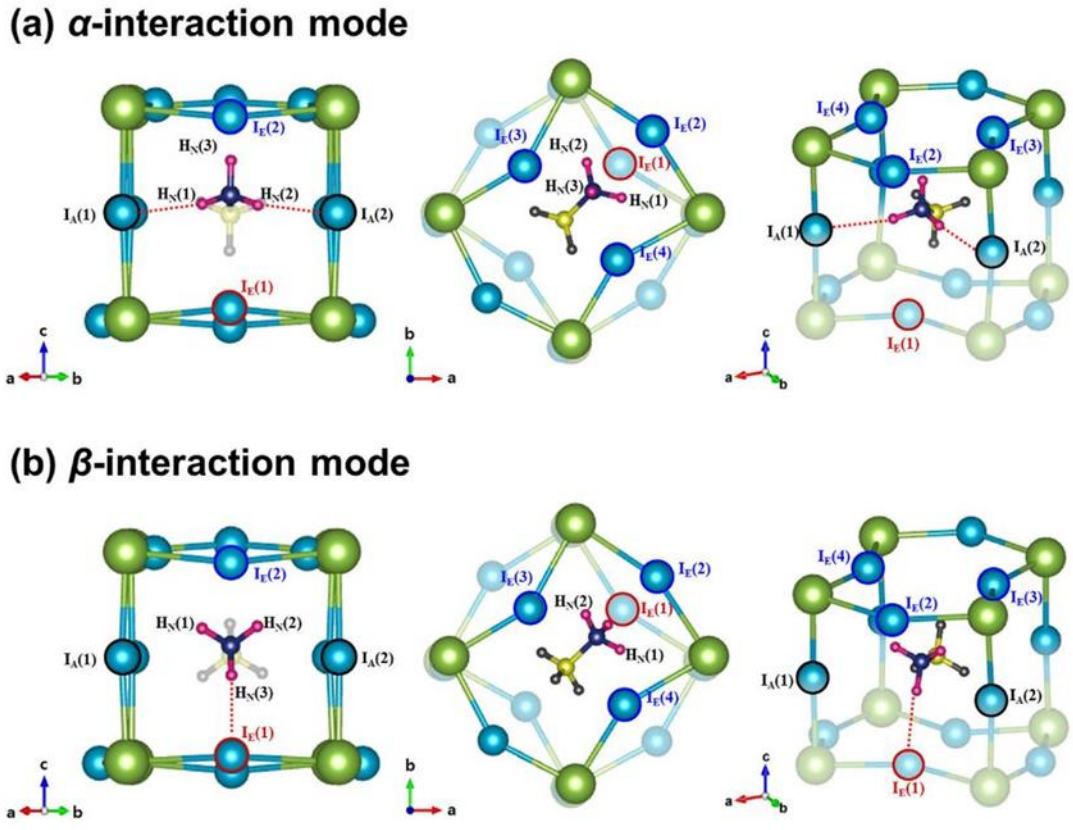

Figure 3. Illustration of the two distinct modes of the hydrogen bonding interaction.[32] Copyright 2016 Springer Nature.

Table 2. The number of hydrogen bonding donors in the cation (n), calculated Total Electrostatic Energies (E_{tot}) and Hydrogen-Bonding Energies ($E_{H\text{-}bond}$) in perovskites with related properties, and the temperature of cation ordering (T_c)[19]

	$MAPbI_3$	$MAPbBr_3$	$MAPbCl_3$	$FAPbI_3$	$FAPbBr_3$	$FAPbCl_3$
n	3	3	3	4	4	4
E_{tot}(eV)	8.59	8.19	9.09	8.60	8.15	9.03
$E_{H\text{-}bond}$(eV)	0.27	0.26	0.26	0.16	0.10	0.09
$E_{H\text{-}bond}$/n(eV)	0.09	0.09	0.09	0.04	0.02	0.02
T_C(K)	173	144	162	140[33]	153[34]	140

The two-dimensional (2D) perovskite structure is composed of a metal halide framework and bulky or long-chain monovalent or divalent organic cations, such as butylammonium (BA), phenethylammonium (PEA), or propyldiammonium (PDA) that acts as a barrier molecule between the inorganic sheets. The structure of 2D perovskite with typically adopted cations and different molecular interactions are shown in Figure 4. 2D perovskites include the Dion-Jacobson (DJ), Ruddlesden-Popper (RP) and alternating-cation-interlayer (ACI) phases. The formulas of these perovskites are $A'A_{n-1}B_nX_{3n+1}$, $A'_2A_{n-1}B_nX_{3n+1}$and $A'A_nB_nX3_{n+1,}$ respectively.[35,36] Hydrogen bonding also plays a key factor in the structure of 2D perovskites. In the RP structure, the long organic cation contains one amino group which can form a hydrogen bond with a metal halide framework. The other side of the long chain interact with adjacent cations via van der Waals interaction. So, the interaction includes hydrogen bonding and van der Waals forces. The hydrogen bonding can affect the coordinating ability of the organic cation toward $[PbI_6]^{4-}$ octahedra as well as the octahedral tilt which contribute the 2D structure.[37,38] In the DJ structure, the long organic cation contains two amino groups at both terminal positions of the long chain. The two amino groups interact with adjacent metal halide frameworks. So there is only hydrogen bonding between the long organic cation and inorganic slabs.[39] Compared to RP perovskites, DJ perovskites eliminate the van der Waals gap by forming hydrogen bonds which lead to a more rigid structure and shortened interslab distance, which can facilitate charge transport and stabilize the layered

perovskite structure.[39,40] In ACI structure, because of the long cation and small cation alternating arrangement, part of the van der Waals gap remains and is embedded in the crystal structure.[41]

2D perovskites show good stability compared to their 3D counterparts.[42] However, the 2D perovskite-based devices show relatively poor efficiency, attributed to the inhibition of out-of-plane charge transport by the organic cations, acting as insulating spacing layers between the conducting inorganic slabs.[42,43] In 2D perovskites, the hydrogen bond plays a key role in regulating the crystal orientation.[44,45] The hydrogen bonding can significantly influence the properties of the perovskite with long-chain organic ammonium.[46] Qin *et al*. realized the reduction of directional dimensionality of perovskites by adjusting the intermolecular hydrogen bonding of organic ammonium.[46] The hydrogen bonding can shorten the distance of inorganic slabs in 2D perovskites, facilitating the charge transport between inorganic slabs in 2D perovskite film.[47,48,49,50] Song et al. showed the hydrogen boding links adjacent spacing sheets leading to the charges localized in the van der Waals gap which constructing "charge-bridge" for charge transfer through the spacing region.[37]

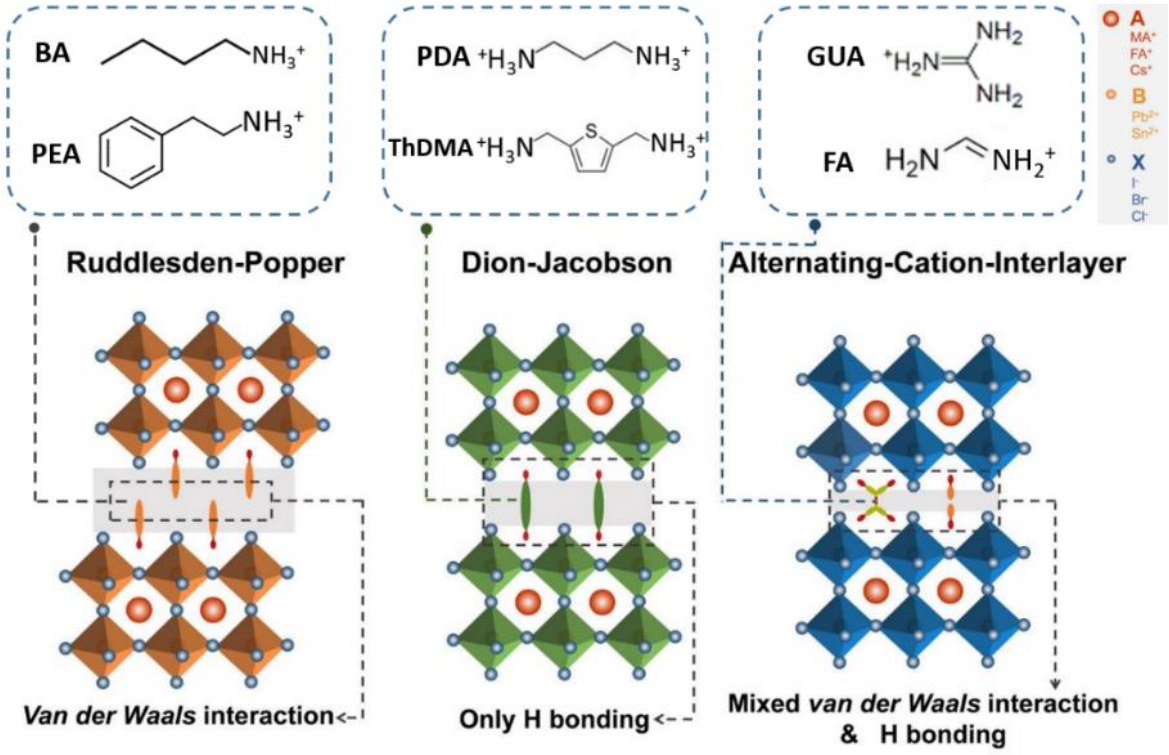

Figure 4. Schematic illustration of 2D perovskite sturctures.[36] Copyright 2022 Wiley-VCH GmbH.

Guanidinium ($C(NH_2)_3$, GUA^+) can be obtained by substituting the hydrogen of C-H in FA^+ with an $-NH_2$ group resulting in three amine groups in the cation.[20] The more hydrogen bond donors comparing MA^+ and FA^+ indicates GUA^+ has more capability to stabilize the structure of perovskite via hydrogen bonding with halide anion. Yu *et al*. utilized the strong hydrogen bonding of GUA^+ with SnI_6^{4+} octahedron to effectively passivate under-coordinated iodide ions and reduce local strains of $FASnI_3$ crystal structure.[51] The hydrogen bonds may lead to local distortions, which can expand the crystal unit.[52] Nazeeruddin *et al*. found a certain amount of GUA^+ replacement of MA^+ result in more hydrogen bonds in perovskite which can stabilize the structure, however, too much GUA^+ will lower the absorption capacity which is indicative of a widening of bandgap.[52]

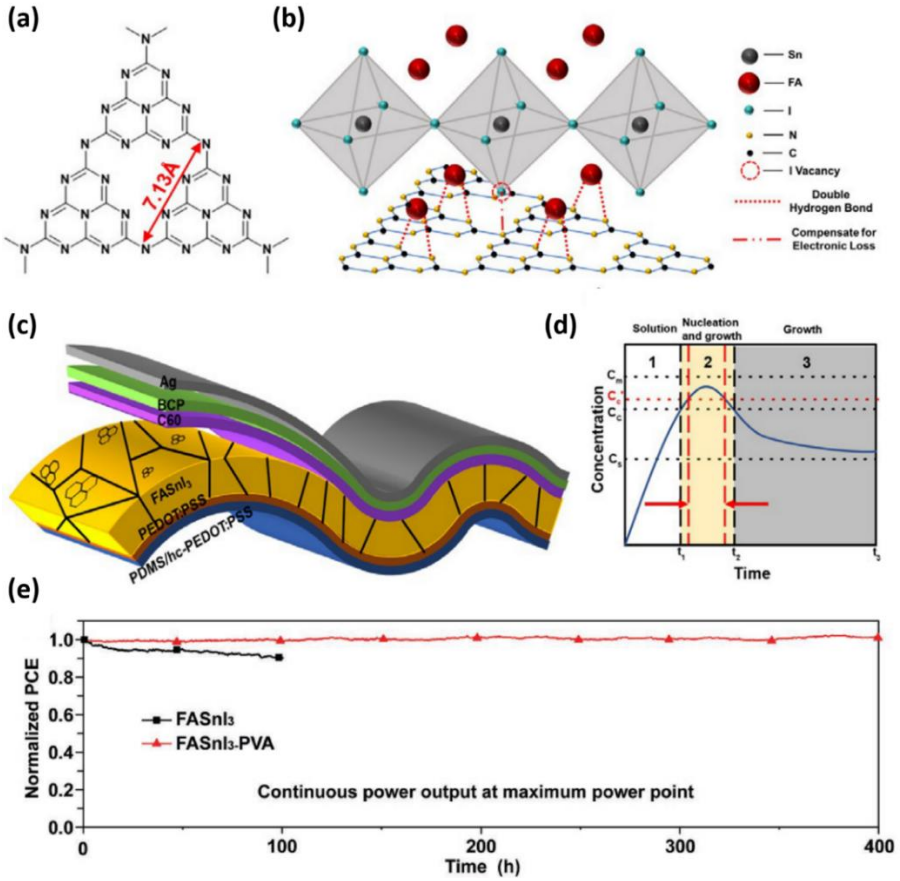

Figure 5. (a) Chemical structural unit of g-C_3N_4. (b) Illustration of bonding and passivation between perovskite and g-C_3N_4. (c) Device configuration. (d) Representation of the different concentration during crystal nucleation and growth according to the LaMer Curve.[57] Copyright 2021, Wiley-VCH GmbH. (e) Device stability.[22] Copyright 2019, WILEY-VCH Verlag GmbH & Co. KGaA, Weinheim.

Tin-based perovskites possess a narrower bandgap than Pb-based perovskites and are promising candidates for bottom cells in efficient PSCs tandems.[22,53,54] However, there are many intrinsic factors such as the facile oxidation of Sn^{2+} to Sn^{4+} easy formation of Sn vacancies can impact the defect chemistry and subsequent recombination of charge carriers which degrade their key optoelectronic properties.[55] In addition, the crystallization rate during annealing of tin-based perovskites is much faster, leading to abundant trap states and much lower V_{oc}. Han *et al*. found that introducing hydrogen bonds via addition of poly(vinyl alcohol) (PVA) can increase nucleation sites, slowing the crystal growth and thus forming a compact $FASnI_3$ film with reduced trap density. Moreover, hydrogen bonds at the grain boundary can suppress migration of the iodide ions which enhanced the stability of devices as shown in Figure 5e.[22] Islam *et al*. successfully implemented a bifunctional compound hydroxylamine hydrochloride (HaHc) into $FASnI_3$ perovskite to reduce the electronic defects by forming a hydrogen bond with iodide ion. The presence of hydrogen bonds suppresses ionic vacancies and stabilize the $FASnI_3$ framework.[56] Chen *et al*. introduced two-dimensional graphite phases-C_3N_4 into tin-based perovskite. The N atoms in the triazine ring coordinate with FA^+ via two hydrogen bonds. The binding site's distance is adjusted to the lattice size of tin-based perovskite, resulting in a suppressed crystal growth rate.[57] The illustration is shown in Figure 5a-d.

Hydrogen bonding affects the properties of perovskite

Hydrogen bonds can affect the optical bandgap and charge transport properties of perovskites.[58] For example, De Angelis *et al*. reported a first principle investigation where they determined that the FA^+ cation has a higher propensity to form hydrogen bonds than MA^+. The enhanced hydrogen bonding between the FA^+ cations and the inorganic matrix alters the Pb-I bond's covalent/ionic character. Moreover, mediated by the different spin-orbit coupling in $FAPbI_3$, the electronic and optical properties can be improved.[58] The strength of hydrogen bonding between $[PbI_6]$ planes and the organic cations affect the band offset in 2D perovskites. [59] A weaker hydrogen bonding usually shifts the bonding states of the bulky organic layer to a higher energy position which brings them closer to the valence band maximum (VBM) of the $[PbI_6]$ planes resulting in a smaller barrier for hole transport between the $[PbI_6]$ inorganic plane and organic cation shown in Figure 6a.

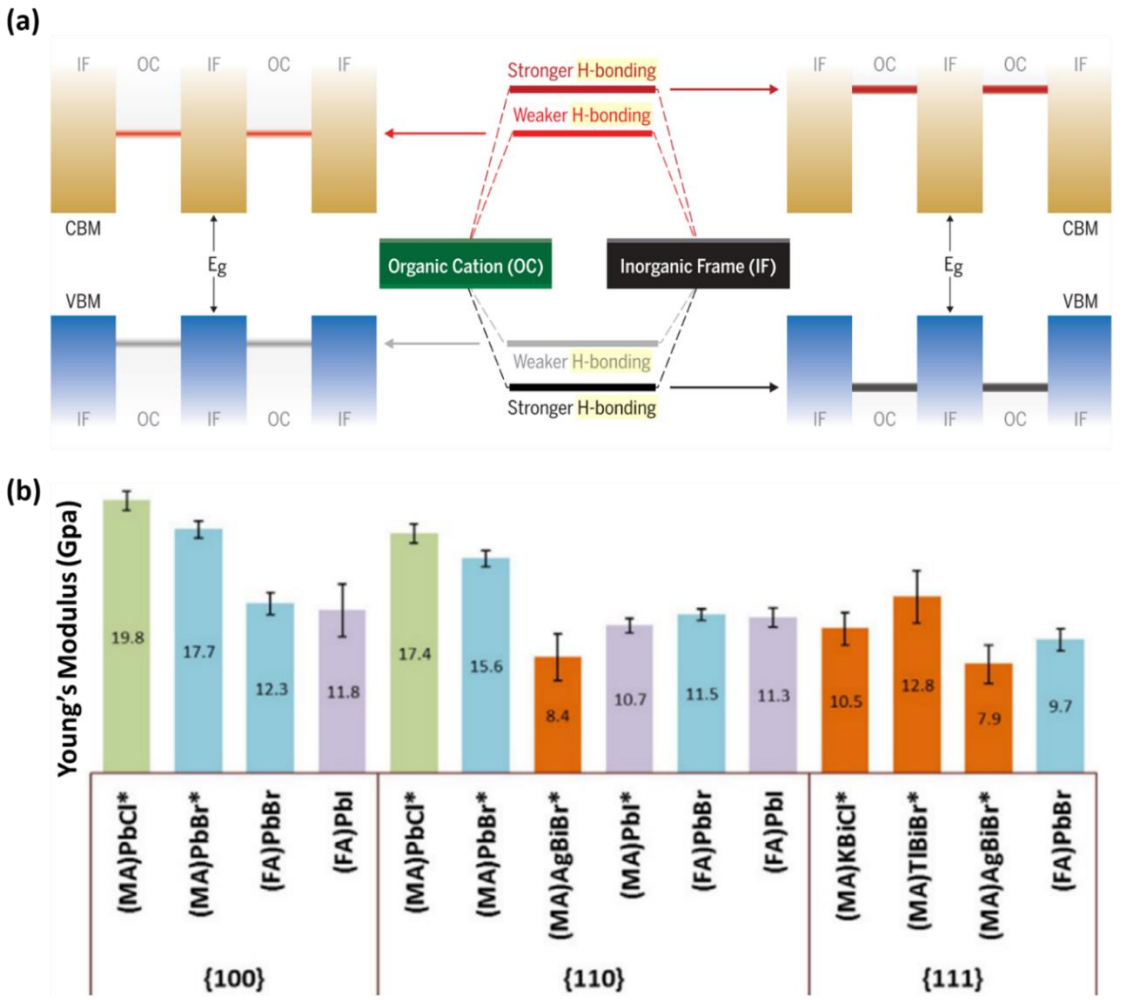

Figure 6. (a) Illustration of the band offsets between [PbI_6] planes and bulky organic cations with a weaker and stronger of hydrogen bonding.[59] Copyright 2022 American Association for the Advancement of Science. (b)Young's moduli of hybrid halide perovskites normal to the {100}, {110}, and {111} planes.[60] Copyright 2017 Wiley-VCH Verlag GmbH&Co. KGaA, Weinheim.

Many studies have shown that hydrogen bonding can influence the orientation of the organic cations and phase transitions.[19,61,62,63] Nan *et al* found the hydrogen bonding is a key factor that affect the motion of organic species further change the surface geometries of perovskite with various defects. And the halide ions movement is largely tuned by the reorientation and rotation of the organic cations with the disruption and formation of the hydrogen bonding. The hydrogen bonding inhibits the formation of light-triggered small exciton-polarons and deep photoinduced traps which cause local structure deformations on the surface of perovskite.[64,65] Cheetham *et al*. used DFT to investigate the thermodynamic effects of hydrogen bonding and its interaction with

the octahedral rotations in the orthorhombic phase $MAPbI_3$.[66] They calculated the rotation energy profile by rotating the NH_3 and CH_3 groups to reflect the strength of the hydrogen bonding. These results indicate that the rotation of staggered MA^+ around its C-N bond is quite difficult because of the strong hydrogen bonding, which results in an activation energy of ~102 meV per MA^+ ion. The hydrogen bonding strength is highly correlated to the octahedral rotations in $MAPbI_3$, which could explain why the MA-ordering transition is consistent with the phase transition temperature.[66] This result is consistent with the finding that hydrogen bonding affects the tilting of the PbI_6^{4-} octahedra. In turn, this is responsible for the relative orientations of the crystal.[31] The length of hydrogen bonds in different phases of $MAPbI_3$ are listed in Table 3. Moreover, hydrogen bonding also affects the mechanical properties of the perovskite.[60] Cheetham *et al*. conducted *ab initio* molecular dynamics (AIMD) to investigate the bonding characteristics on the elastic properties.[60] They first measured the Young's moduli and hardness of $FAPbX_3$ ($X=Br^-$ or I^-) experimentally, then calculated the pairwise Radial Distribution Functions (RDF) using AIMD. The RDF results revealed that the hydrogen bonding is stronger in $MAPbBr_3$ than $FAPbBr_3$, which caused the higher mechanical stability of the former one. Their results shown that hydrogen bonding plays important roles in determining elastic stiffness, as shown in Figure 6b. The elastic properties impact how the material deals with mechanical stress, which impacts recombination.[67]

Walker et al. investigated mixed-cation iodide perovskites using AIMD simulation.[68] They found that mixed-cation increased the N-H···I hydrogen bond. This stronger hydrogen bonding is supposed to increase the phase-stability of mixed-cation perovskites. Islam et al. further investigated perovskites $FA_{1-x}Cs_xPbI_3$ with $x \leq 0.25$. They found that the FA^+ orientations only result in small differences in the energy. Introducing Cs^+ can induce a chemical pressure or lattice strain effect through Cs/FA ion size mismatch which then increase the N-H···I bond strength. This then helps the thermal stability of the mixed cation perovskites. In this study, the strength of hydrogen bonding is also evaluated using the non-covalent interactions index which employs the electron density and its derivatives to identify the noncovalent bonds.[69]

As mentioned, hydrogen bonds have tunable strength and directionality. There can be many positive influences introduced by hydrogen bonding in PSCs. The hydrogen bonding can stabilize the perovskite by inhibiting both the volatilization of the organic cations and ion migration.[70] The volatile nature of organic species (e.g. FA^+, MA^+, etc.) is a key factor for the degradation in hybrid perovskites, particularly under thermal stability testing[71,72]. Hydrogen bonds between

Table 3. The length of hydrogen bonds in $MAPbI_3$

Phase	Orthorhombic		Tetragonal		Cubic	
Bond position*	HB^{a}_{Ortho}	HB^{b}_{Ortho}	HB^{a}_{Tetra}	HB^{b}_{Tetra}	HB^{a}_{Cubic}	HB^{b}_{Cubic}
Length(Å)	2.613	2.808	3.184	3.394	3.120	3.520

*The detailed position of hydrogen bonds in $MAPbI_3$ can be found in Ref.[61]

FA/MA species suppress their volatilization and improve device stability.[73] Fang *et al*. introduced an additive with alkoxy (–O–CH_2) and hydroxyl (–OH) groups, forming hydrogen bonds with organic cations. The strong interaction inhibited the volatilization of the organic cation, improving device stability.[73] Zhao *et al*. introduced poly(ethylene glycol (PEG)-based polymer-scaffold architecture into the perovskite film. Hydrogen bonding anchors the entangled PEG molecules on the surface of perovskite grains. Two kinds of hydrogen bonds were formed: $OH^{\cdots}I$ and $NH^{\cdots}O$. Due to the hydrogen bonding, PEG can anchor and inhibit the loss of MAI. These interactions improved the stability via a self-healing effect of the device.[74] Hu *et al*. observed a similar self-healing phenomenon, where they introduced N-$H^{\cdots}O$ hydrogen bonding interactions by adding polyvinylpyrrolidone into $MAPbI_3$.[21] Chen *et al*. introduce a fluorinated perylene diimide (F-PDI) into the perovskite film. The strong hydrogen bonding between fluorine groups and MA^+ (N-H⋯F) can immobilize MA^+ to retard crystallization rate and ensure astonishing thermal stability. Furthermore, the inhibition of decomposition prevents iodine diffusion and reaction with the silver electrode.[75] The schematic illustration of the interaction is depicted in Figure 7.

Ion migration in perovskites is considered one of the critical reasons for device degradation, which can cause hysteresis, induce defects, phase segregation, and even damage the adjacent functional layers.[73,76] By embedding hydrophobic fluorinated-gold-clusters in the perovskite layer, the fluorine groups can form hydrogen bonds with the perovskite, inhibiting ion migration and improving thermal and operational stability.[23] Gong *et al*. have shown the hydrogen bonding between halide anion and organic cation can passivate the ions at the crystal boundaries and reduces the point defects then shield perovskite from exotic moisture and oxygen attack.[77] Fang *et al*. introduced dipentaerythritol pentaacrylate into their perovskite films, and the hydrogen bonding between alkoxy (-O-CH_2) / hydroxyl (-OH) and -NH inhibited I^- ion migration, resulting

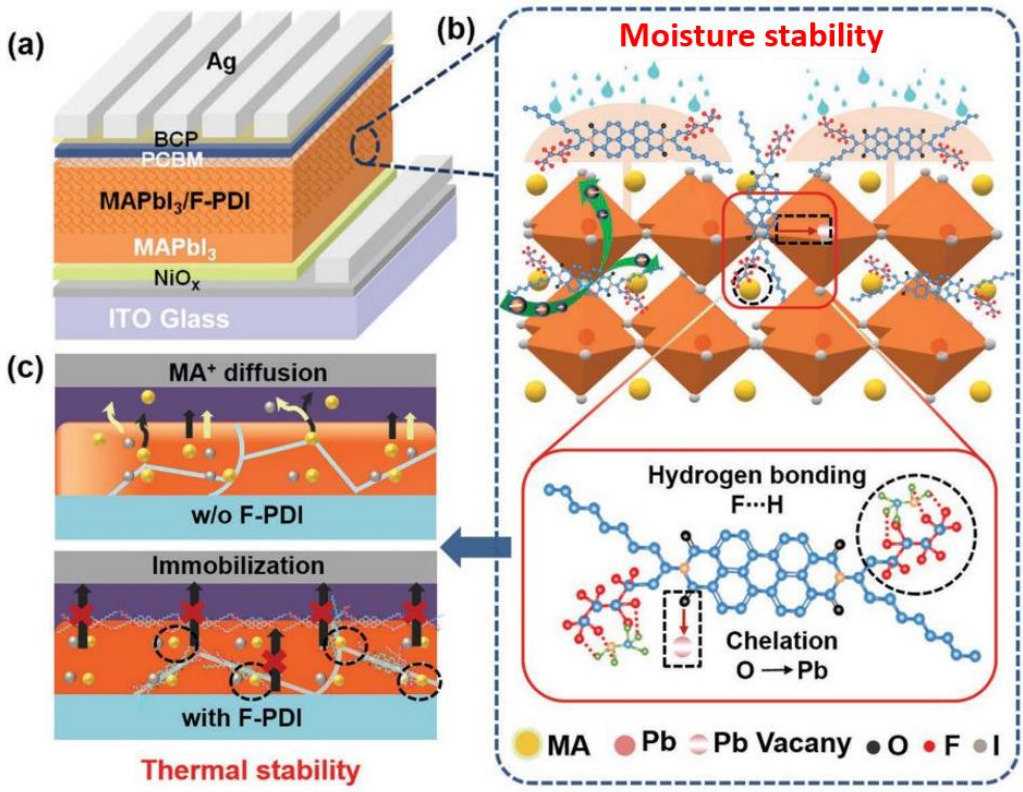

Figure 7. (a) Device architecture. (b) Schematic illustration of the interaction. (c) Schematic diagram of thermal degradation for perovskite [75] Copyright 2019, WILEY-VCH Verlag GmbH & Co. KGaA, Weinheim.

in enhanced device stability, particularly under thermal conditions.[73] Mohammed *et al.* used DFT to investigate the effects of hydrogen bonds on the halogen vacancy and interstitial migration properties.[66] They found that hydrogen bonding in the *nonsymm*-$FAPbBr_3$ is stronger than the *symm*-$FAPbBr_3$. The *nonsymm*-$FAPbBr_3$ has the largest hydrogen bond energy and the shortest H···Br which is further confirmed by an organic cation rotation profile calculated using Nudged Elastic Band method. They also calculated halogen vacancy migration barriers, and concluded that strong hydrogen bonding prevents ion migration and therefore improves the performance of PSCs.

Moreover, the hydrogen bonds at the grain boundary also suppress the iodide migration.[22] Iodine vacancies and under-coordinated Pb^{2+} on the surface of perovskite films are mainly responsible for non-radiative charge recombination. Hydrogen bonding can minimize the number of under-coordinated Pb^{2+} and Pb clusters and passivate the iodide vacancy defects facilitating the charge transport.[78] Chen *et al*. employed carbon nanodots with rich carboxylic acid and hydroxyl

groups, which interact with the perovskite through hydrogen bonds, and promote improvement in carriers' lifetime.[79]

Hydrogen bonding in the electron transport layer

A high-quality electron transport layer (ETL) is formed from an n-type material with a suitable energy level, high electron mobility and good uniformity/coverage.[80,81] Introducing hydrogen bonding into the ETL has been demonstrated to be an effective strategy to improve the quality of the ETL itself. Huang *et al*. applied a C_{60}-substituted benzoic acid self-assembled monolayer (C_{60}-SAM) to form hydrogen bonding with crosslinking agent Tri-chloro(3,3,3-trifluoropropyl)silane.[82] The hydrogen bonds align the C_{60}-SAM molecules in order instead of

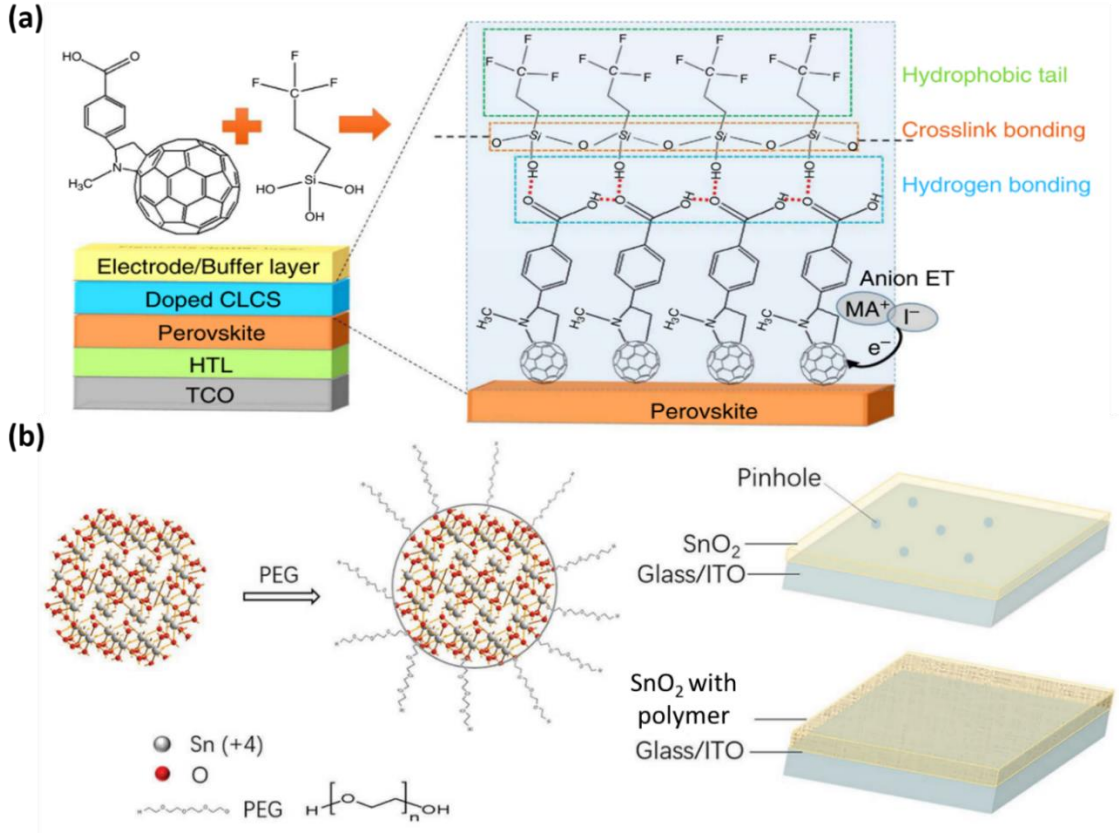

Figure 8. (a) Device structure and schematic illustration for the crosslinking.[82] Copyright 2016, Springer Nature. (b) Schematic illustration of the interaction between SnO_2 and PEG, and the diagram of the morphology of the SnO_2 film.[83] Copyright 2018, WILEY-VCH Verlag GmbH & Co. KGaA, Weinheim.

randomly forming dimers driven by the silane crosslinking process. The resulting pseudo-polymer structure makes the film more uniform and compact and after enhances ETL's electron mobility. The crosslinking mechanism is illustrated in Figure 8a. Polymer molecules can act like ligands surrounding the inorganic nanoparticles, so polymer additives to the electron transport materials precursor is an effective way to inhibit the aggregation of nanoparticles which cause the pinholes and nonuniformity.[83,84] Xu *et al*. incorporated polyethylene glycol (PEG) into the SnO_2 colloid.[83] The strong hydrogen bonding between PEG and SnO_2 nanoparticles disaggregates the SnO_2 oligomers, whereby a dense and uniform ETL with ultrathin thickness is formed due to the improved dispersity of the SnO_2 precursor solution. The schematic diagram is shown in Figure 8b. Introducing hydrogen bonding into ETLs would be an ideal strategy to tailor the morphology and electronic structure which further influence the charge transport.

Hydrogen bonding in the hole transport layer

The hole transport layer (HTL) in PSCs must meet general criteria such as suitable energy level, reasonable hole mobility and good stability.[85,86] Small molecular materials are the common hole transport materials used in PSCs.[86] The adjacent molecular packing significantly affects the charge carrier mobility and if the materials exhibit self-assembling properties that can effectively increase the mobility.[87] So during the synthesis process, hydrogen bonds could be a multifunctional tool to optimise the properties rather than using additives which is usually detrimental for the stability.[88] Islam *et al*. found that a tetrathiafulvalene derivative containing two amide units can form self-assembled supramolecular structures via intermolecular hydrogen bonds. The corresponding film shows higher conductivities than spiro-OMeTAD.[89] Zhang *et al*. demonstrate that hydrogen bonding interactions can significantly increase the hole mobility and form Pb–N coordination bonds at the interface to promote hole extraction via studying the dopant-free hole transport material.[90] Their research results showed that the hole mobility of the hole transport material (HTM) increased from 1.11×10^{-4} to 3.09×10^{-4} $cm^2\ V^{-1}\ s^{-1}$ ascribed to the hydrogen bonding interaction, resulting in a significantly enhanced performance of the device. Moreover, they demonstrate that rational design of HTM can self-assemble into a long-range ordered interlayer on the interface between the perovskite and HTL by hydrogen bonding interaction as depicted in Figure 9a. Thus hydrogen bonding would be a versatile multi-functional tool for the design of the class of small self-assembling HTM molecules which are becoming more

mainstream.[88] Hagfeldt *et al*. proposed a strategy to synthesise high-quality NiO_x nanoparticles as HTMs via $[BMIm]BF_4$ ionic liquid additive engineering.[91] The cations of $[BMIm]^+$ can form a strong hydrogen bond with nickel hydroxide, which inhibit the adsorption of impurity ligand NO_3^- in NiO_x in HTL and slow down the interfacial degradation reaction. As a consequence, the target NiO_X HTL enabled a high PCE up to 22.6% with negligible *J-V* hysteresis and significantly improved device stability as show in Figure 9b and c.

Hydrogen bonding at the interface

The interface plays a crucial role in the device. Interfacial charge recombination is one of the dominant loss mechanisms in PSCs. Rational interface optimization is considered an effective strategy to improve the performance of PSCs.[92,93,94,95] The hydrogen bonding can enhance the adhesion of perovskite and charge transport layers. Sin *et al*. added a polar insulating polymer, poly(ethylene glycol) (PEG), into the ETL. The ETL with PEG retains perovskite with hydrogen

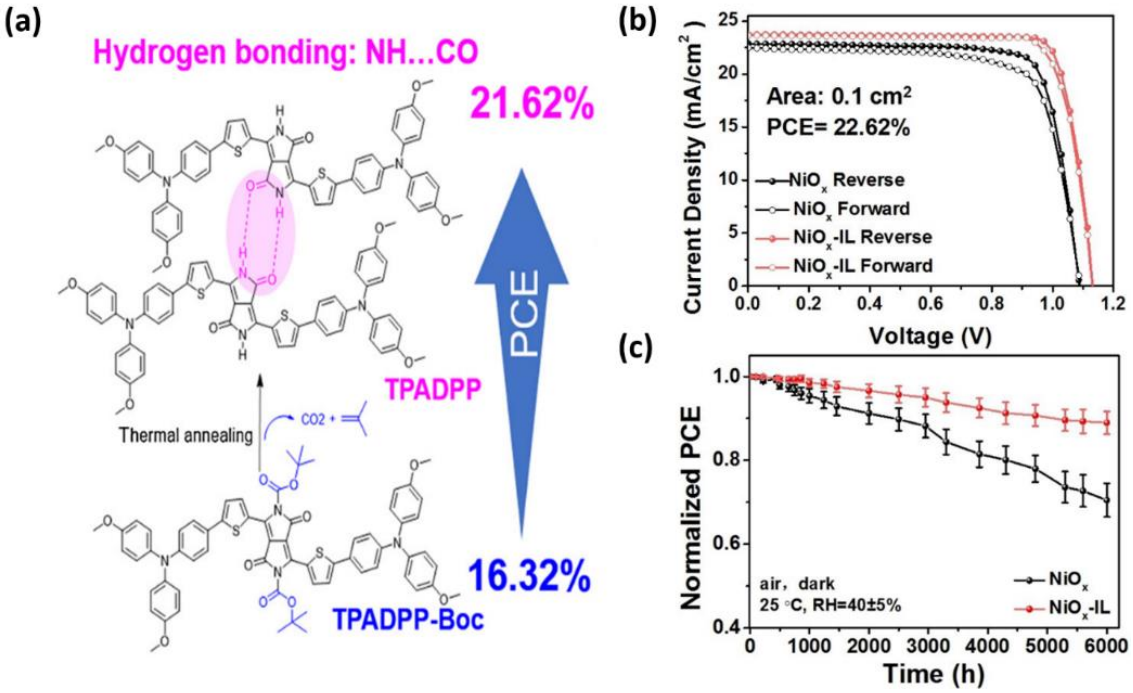

Figure 9. (a) Chemical structures of materials and illustration of the hydrogen-bonding formation.[90] Copyright 2021, Chinese Chemical Society. (b) *J–V* characteristics of the devices. (c) PCE stability of the devices storaged in dark and ambient air with relative humidity 40 ± 5%.[96] Copyright 2022, Wiley-VCH GmbH.

bonding during the perovskite formation, resulting in better contact between the ETL and perovskite layer.[97] Li *et al*. incorporated NaX (X = halide series) at 0.1 mol% in a PbI_2 precursor film for sequential perovskite deposition.[98] The most electronegative F^- ion was observed to form N-H···F hydrogen bonds with the alkylammonium cations. Depth profiling studies showed the F- ions accumulated at the perovskite/charge transport layer (CTL) interfaces, resulting in stabilization of the perovskite surface and suppressed formation of cation vacancies. These devices showed a pronounced increase in thermal- and photo-stability compared to the other halides, confirming the efficacy of the hydrogen bond stabilization. Interestingly, p-i-n devices often use ultra-thin evaporated fluoride salts (e.g., LiF, MgF_x etc) to increase the selectivity of the perovskite/ETL interface.[99] It is an open question whether these interfaces further benefit from hydrogen bonding in the same manner.

A recent strategy to boost performance and stability is the inclusion of a bulky salt (or ionic liquid) into the perovskite precursor solution at a few mol% relative to Pb. The oversized organic cations and anions are excluded from the bulk perovskite, and reside at grain boundary interfaces.[100,101]The tetrafluoroborate anion (BF_4^-) is commonly used, and while the species is considered inert from a Lewis base perspective, it is known to undergo hydrogen bonding.[102] (including in related molecular hybrid perovskites).[103] The mechanism of BF_4^- anion was recently attributed to iodide management, reducing deep trap states originating from excess MAI through a direct reaction with $MABF_4$ as a co-crystal.[104] The interaction has H-bond characteristics, with decreased ^{11}B-^{19}F NMR coupling (which is known to be H-bonding dependent[105]) and a blue-shift in XPS consistent with H-bonding driving co-crystal formation.[25]

Indeed, it is likely that interfacial hydrogen bonding is often present in passivated devices, but its effects are often overlooked. The rear perovskite/CTL interface is commonly passivated with polar molecular passivating agents. It seems reasonable to hypothesize that hydrogen bonding will be present, particularly as some of these passivating agents have known hydrogen-bonding properties when applied in different fields. For example, Zheng *et al*. used choline chloride to passivate the rear interface of p-i-n perovskites, boosting performance and stability.[106] This reagent is well known to the deep eutectic solvent community, where a 1:2 molar ratio of choline chloride and urea forms a classical deep eutectic solvent with a low melting point.[107] Page *et al.* used Density Functional Tight Binding calculation to investigate the deep eutectic solvent structures and interactions, and show that the quaternary ammonium within choline chloride acts as a

hydrogen bond acceptor determining the melting point and viscosity properties of the deep eutectic solvent.[108] We highlight this as an example similar to the guanidinium case, the hydrogen bonding properties are well established in other fields, yet largely overlooked by our field. Given the commonplace reports of molecular interface passivation, we urge readers to consider the effects of hydrogen bonding on device performance and stability.

Computational chemistry for hydrogen bonding in perovskite solar cells

Computational calculation is also a powerful tool to investigate the hydrogen bonding interaction, such as DFT calculation,[19] AIMD, etc.[60,109] It calculates properties related to hydrogen bonding and provides theoretical explanations and mechanical insights for the functionality of the hydrogen bonding in the perovskite solar cells. However, *ab initio* methods treat the energy term as a function of the entire system without modelling the individual contributions such as the hydrogen bonding explicitly. The contribution of hydrogen bonding to the perovskite's properties is thus inferred as an additional step in practice when required. The most commonly used metric is hydrogen bond distance. In the simplest computational chemistry tool, force field[110], the non-bonded term is usually approximated by a combination of van der Waals interactions and electrostatic interactions, as

$$E_{non-bonded} = \frac{A}{r^{12}} - \frac{B}{r^{6}} + \frac{q_i q_j}{\epsilon r}$$

where A, B, q_i, q_j are force field parameters, and r is the distance between two atoms. Although force field is mostly used in biological systems and seldomly used for materials such as perovskites, it provides us with the intuition that the shorter the distance is, the higher the energy and stronger the bond strength. It was also suggested that the heavy-atom distance can be used as an indicator of hydrogen bonding strength.[111] As emphasized, the energy of hydrogen bonding cannot be calculated directly in DFT, and must be estimated using some approximations. The simplest way is comparing the energy differences between an organic cation system and an inorganic cation system, which removes the monopole term in the electrostatic interactions and obtains an energy term focused on the hydrogen bond.[19] An empirical approximation based on bond critical point has been used as well.[112] These methods need to calculate the electron density along the bonding direction, which means higher levels of theory (e.g. DFT with level of meta-GGA[113]) can improve the accuracy, with the cost of higher computational burden. Rotational profile which shows the

energy as a function of the organic cation rotation angle has also been used to estimate hydrogen bonding energy.[114]

Detrimental effects of hydrogen bonding in PSCs

Hydrogen bonding can work as a double-edged sword for the performance of PSCs. And another detrimental influence of hydrogen bonds can be introduced by water. The halide perovskite is notorious due to its sensitivity to moisture. Moisture plays a key role in perovskite formation, phase transition and degradation.[115,116,117,118] Water molecules can penetrate the perovskite lattice and share the space with organic cation. The hydrogen bonding between the water H-atoms and the N atom of organic cation enhances the formation a hydrate intermediate, such as $(CH_3NH_3)_4PbI_6 \cdot 2H_2O$, which is the first step in the perovskite decomposition process. Sit et al.[119] used DFT to investigate the stability of perovskite with the presence of water molecular at the interface, and found that hydrogen bonds were formed between the oxygen of the water and the hydrogen in the NH_3 group, and the existence of O···H breaks some of the H···X (X is the halide ion) bonds. In the presence of OH radicals, a hydrogen atom will transfer from the MA^+ cation to form a H_2O and a CH_3NH_2 molecules. Given these results, strengthening the hydrogen-bonding interaction between the organic cation and metal halide octahedra and/or weakening the hydrogen interaction between the organic cation and H_2O could improve moisture resistance of the perovskite. It is worth noting, Bao *et al*. found that for the $MAPbI_3$ perovskite, the interaction between MA and H_2O through hydrogen bonding is not established until the phase transition to monohydrate, where H_2O and MA are locked to each other. Water absorption in ambient air (25 °C and 40−45% relative humidity) is negligible, however, significant water absorption is observed only when the RH reaches ∼85%.[115] Heben *et al*. revealed the degradation process caused by water can be described as a four-stage process and three of them are reversible.[120] However, a moderate amount of water in perovskites is found to facilitate the nucleation and crystallization process of the perovskite, resulting in a better quality film[121,122] and the water additive in ETL can shape the architecture to improve light-scattering for the enhancement of performance.[123]

Adjusting/controlling the hydrogen bonding in PSC

The research discussed above shows that introducing hydrogen bonds in a targeted amount and position is an effective strategy to improve PSC performance. The configuration of the

hydrogen bonding in PSC is highly complicated. It is challenging to control hydrogen bonding precisely. In view of intrinsic stability of perovskite, it would lead to numerous local minima in the potential energy surfaces. Thus, it would be extremely difficult to find the optimum configuration. The normal strategies to build new hydrogen bonds is to add hydrogen bond donor and/or acceptor into perovskite materials.[124] An indirect method has been demonstrated by Islam *et al*., where they found that incorporating Cs^+ cation into the $FAPbI_3$ structure can induce a chemical pressure or lattice strain effect through Cs/FA ion size mismatch. This results in structural distortion that strengthens the FA-iodide (N−H···I) hydrogen bonding interaction.[109] Both Jen *et al*. and Qin *et al*. utilized the hydrogen bonding introduced by the additive to modulate the crystal nucleation and film-forming processes. They found the hydrogen bonding could adjust the crystallization kinetics and complex intermediate phase to obtain a high-quality perovskite film. [1617] The schematic of hydrogen bonding assisted perovskite film growth is shown in Figure 10.

In 2D perovskites, we can manipulate the long-chain organic spacer to optimize the intermolecular hydrogen bonding interaction. The structure of organic cations, the growth condition and the functional group in cation can all contribute to the properties of hydrogen bonds further affect the properties of the perovskite. Zhu *et al*. discussed that a DJ structure perovskite with weaker hydrogen bonding should improve hole transport; however, a weaker hydrogen bonding configuration generally means a less stable structure.[59] Thus, hydrogen-bonding must be balanced between the high-efficiency band and high stability in PSCs. Hartono et al. used machine learning to optimize the capping layer to increase the stability of their PSCs.[125] They applied 21 organic halide salts as capping layers onto $MAPbI_3$ and used machine learning algorithms to determine the most important features that correlate with stability. They found that low number of hydrogen bonding donors of the organic cations and small topological polar surfaces area are the two most important features that correlate with stability. Their results support the hypothesis that hydrogen bonding plays a crucial role in the degradation of PSCs. Wheeler *et al*. controlled the hydrogen bonding via exposure to solvent vapor and temperature change realized a reversible multicolor chromism.[126] Hydrogen bonds can also be introduced in other ways, such as through the use of the antisolvent. Jung *et al*. used anisole as an antisolvent due to the intermolecular hydrogen bonding forces between anisole and DMF/DMSO, where an ultrawide processing window to fabricate high-quality perovskite films was realized.[127]

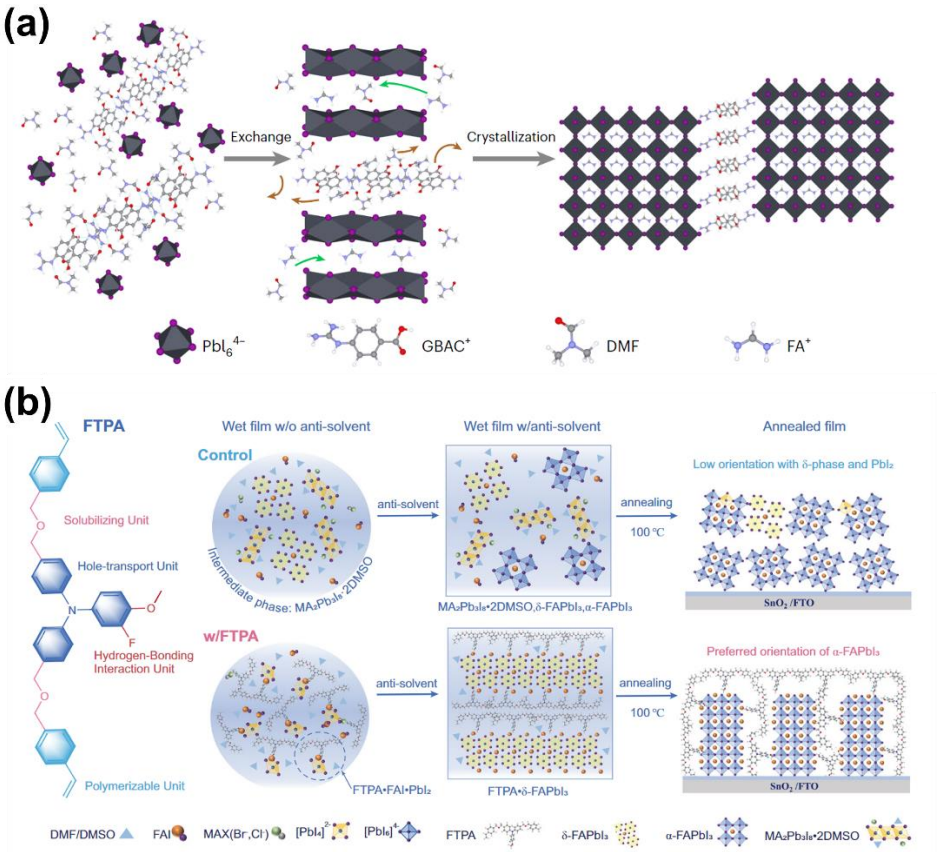

Figure 10. The schematic diagram of hydrogen bonding assisted perovskite film growth.[16,17] Copyright 2023 Springer Nature.

Summary and outlook

In this review, we discussed the weak molecular interaction of hydrogen bonding in PSCs, including the effects of hydrogen bonding in each functional layer and interface. Hydrogen bonding can act as a double-edged sword in PSCs. On the one hand, hydrogen bonds can stabilize the perovskite materials by inhibiting the organic cation volatilities and ion migration, enhanced the charge transport, and inhibiting the charge recombination. However, on the other hand, hydrogen bonding has also been shown to accelerate perovskite degradation by enhancing the interaction with water. Thus, the function of the hydrogen bond is versatile, as show in Figure 11. Retarding the crystal growth results in uniform nucleation producing homogeneous and pinhole free film with reduced trap density. Affecting the order-disorder transition mechanism which is related to the phase stability of the perovskite. We also briefly introduce the characterization of

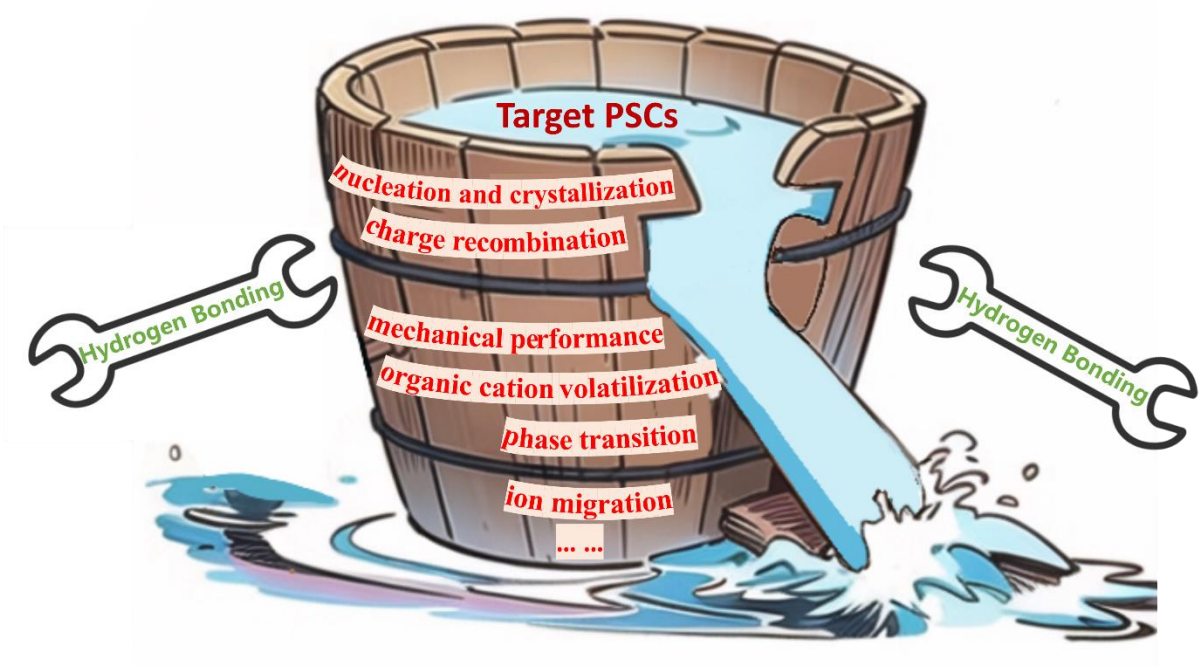

Figure 11. Hydrogen bonding as a versatile tool.

hydrogen bonding. Experimental techniques and calculations are a powerful combination for quantifying the strength of hydrogen bonding. However, optimization of the method in calculation is still necessary. That would ensure the calculation results are more consistent with the experimental results. Finally, we discussed how to control the hydrogen bonds to make them beneficial for improving the performance of PSCs. Research has shown introducing hydrogen bonding in the molecular design concept, such as amine units, is a simple and effective strategy to develop high-performance hole transport materials. More effort needs to be made for developing new strategies to precisely control the hydrogen bonding in materials to obtain the target properties in the future work.

We observe in the literature that the research on hydrogen bonding in PSC is still controversial and poorly understood. As such, an important consequence of hydrogen bonding of asymmetric alkylammonium cations is orbital splitting via the so-called Rashba-effect.[128,129,130,131] Studies of Rashba-type effects in perovskites are still in their early stages, further investigation of hydrogen bonding will uncover interesting features affecting device performance and stability. We anticipate this review can raise the profile of the various effects of hydrogen bonding in PSC, as it is likely often overlooked. We further anticipate PSC researchers can harness hydrogen bonding as a versatile multi-functional tool, to solve the challenges of commercialization of PSCs.

Author contributions

L. L conceived the framework of the review. L. L and T. C. J. Y. researched data for the article. X. L. and J. Q. S. drafted the computational chemistry and machine learning related parts. X. W, G. W and S.S directed this project. All authors discussed the content and contributed to the writing of the manuscript.

Declaration of interests

SDS is a co-founder of Swift Solar.

Acknowledgement

This work was supported by the Natural Science Foundation of Hubei Province of China (202211301201002), Wuhan Municipal Science and Technology Bureau of China (202211301251333). L.L thanks the support from "Program of Overseas Expertise Introduction Center for Discipline Innovation" and Shihao He for the modification of the figures.

References:

1. Best Research-Cell Efficiency Chart | Photovoltaic Research | NREL. https://www.nrel.gov/pv/cell-efficiency.html.
2. Cheng, Y., Ding, L. (2021). Pushing Commercialization of Perovskite Solar Cells by Improving Their Intrinsic Stability. Energy Environ Sci *14*, 3233–3255. 10.1039/D1EE00493J.
3. Ma, S., Yuan, G., Zhang, Y., Yang, N., Li, Y., and Chen, Q. (2022). Development of encapsulation strategies towards the commercialization of perovskite solar cells. Energy Environ Sci *15*, 13–55. 10.1039/D1EE02882K.
4. Min, H., Lee, D., Kim, J., Kim, G., Lee, K., Kim, J., Paik, M., Kim, Y., Kim, K., Kim, M., Shin, T., and Seok S. (2021). Perovskite solar cells with atomically coherent interlayers on SnO_2 electrodes. Nature *598*, 444–450. 10.1038/s41586-021-03964-8.
5. Zhu, M., Li, C., Li, B., Zhang, J., Sun, Y., Guo, W., Zhou, Z., Pang, S., and Yan.Y., (2020). Interaction engineering in organic–inorganic hybrid perovskite solar cells. Mater Horiz *7*, 2208–2236. 10.1039/D0MH00745E.
6. Metrangolo, P., Canil, L., Abate, A., Terraneo, G., and Cavallo, G. (2021). Halogen Bonding in Perovskite Solar Cells: A New Tool for Improving Solar Energy Conversion. Angewandte Chemie *61*, e202114793. 10.1002/anie.202114793.
7. Vladilo, G., and Hassanali, A. (2018). Hydrogen bonds and life in the universe. Life *8*, 1–22. 10.3390/life8010001.
8. Sun, C.Q., Zhang, X., Fu, X., Zheng, W., Kuo, J., Zhou, Y., Shen, Z., and Zhou, J. (2013). Density and Phonon-Stiffness Anomalies of Water and Ice in the Full Temperature Range. J Phys Chem Lett *4*, 3238–3244. 10.1021/jz401380p.
9. Xie, J., Liang, Z., and Lu, Y.C. (2020). Molecular crowding electrolytes for high-voltage aqueous batteries. Nat Mater *19*, 1006–1011. 10.1038/s41563-020-0667-y.
10. Yamada, Y., Usui, K., Sodeyama, K., Ko, S., Tateyama, Y., and Yamada, A. (2016). Hydrate-melt electrolytes for high-energy-density aqueous batteries. Nat Energy *1*, 16129. 10.1038/nenergy.2016.129.
11. Mason, P.E., Neilson, G.W., Enderby, J.E., Saboungi, M.-L., Dempsey, C.E., MacKerell, A.D., and Brady, J.W. (2004). The Structure of Aqueous Guanidinium Chloride Solutions. J Am Chem Soc *126*, 11462–11470. 10.1021/ja040034x.
12. Arunan, E., Desiraju, G.R., Klein, R.A., Sadlej, J., Scheiner, S., Alkorta, I., Clary, D.C., Crabtree, R.H., Dannenberg, J.J., Hobza, P., et al. (2011). Definition of the hydrogen bond (IUPAC Recommendations 2011)*. Pure and applied chemistry *83*, 1637–1641. 10.1351/PAC-REC-10-01-02.

13. Hibbert, F., and Emsley, J. (1990). Hydrogen bonding and chemical reactivity. Adv Phys Org Chem *26*, 255–379. 10.1016/S0065-3160(08)60047-7.
14. Thomas, S. (2002). The Hydrogen Bond in the Solid State. Angewandte Chemie International Edition *41*, 48–76.
15. Shahi, A., and Arunan, E. (2016). Why are Hydrogen Bonds Directional ? Journal of chemical sciences *128*, 1571–1577. 10.1007/s12039-016-1156-3.
16. Li, F., Deng, X., Shi, Z., Wu, S., Zeng, Z., Wang, D., Li, Y., Qi, F., Zhang, Z., Yang, Z., Jang, S., Lin, F., Tsang, S., Chen, X., and Jen, A., (2023). Hydrogen-bond-bridged intermediate for perovskite solar cells with enhanced efficiency and stability. Nat Photonics *17*, 478–484. 10.1038/s41566-023-01180-6.
17. Li, M., Sun, R., Chang, J., Dong, J., Tian, Q., Wang, H., Li, Z., Yang, P., Shi, H., Yang, C., Wu, Z., Li, R., Yang, Y., Wang, A., Zhang, S., Wang, F., Huang, W., and Qin, T., (2023). Orientated crystallization of FA-based perovskite via hydrogen-bonded polymer net- work for efficient and stable solar cells. Nat Commun *14*, 573. 10.1038/s41467-023-36224-6.
18. Li, X., Ibrahim Dar, M., Yi, C., Luo, J., Tschumi, M., Zakeeruddin, S.M., Nazeeruddin, M.K., Han, H., and Grätzel, M. (2015). Improved performance and stability of perovskite solar cells by crystal crosslinking with alkylphosphonic acid ω-ammonium chlorides. Nat Chem *7*, 703–711. 10.1038/nchem.2324.
19. Svane, K.L., Forse, A.C., Grey, C.P., Kieslich, G., Cheetham, A.K., Walsh, A., and Butler, K.T. (2017). How Strong Is the Hydrogen Bond in Hybrid Perovskites? Journal of Physical Chemistry Letters *8*, 6154–6159. 10.1021/acs.jpclett.7b03106.
20. Kubicki, D.J., Prochowicz, D., Hofstetter, A., Saski, M., Yadav, P., Bi, D., Pellet, N., Lewiński, J., Zakeeruddin, S.M., Grätzel, M., and Emsley, L., (2018). Formation of Stable Mixed Guanidinium-Methylammonium Phases with Exceptionally Long Carrier Lifetimes for High-Efficiency Lead Iodide-Based Perovskite Photovoltaics. J Am Chem Soc *140*, 3345–3351. 10.1021/jacs.7b12860.
21. Niu, Y., He, D., Zhang, Z., Zhu, J., Gavin, T., Falaras, P., and Hu, L. (2022). Improved crystallinity and self-healing effects in perovskite solar cells via functional incorporation of polyvinylpyrrolidone. Journal of Energy Chemistry *68*, 12–18. 10.1016/j.jechem.2021.10.029.
22. Meng, X., Lin, J., Liu, X., He, X., Wang, Y., Noda, T., Wu, T., Yang, X., and Han, L. (2019). Highly Stable and Efficient FASnI3-Based Perovskite Solar Cells by Introducing Hydrogen Bonding. Advanced Materials *31*, 1903721. 10.1002/adma.201903721.

23. Guo, P., Zhu, H., Zhao, W., Liu, C., Zhu, L., Ye, Q., Jia, N., Wang, H., Zhang, X., Huang, W., Vinokurov, V., Ivanov, E., Shchukin, D., Harvey, D., Ulloa, J., Hierro, A., Wang, H., (2021). Interfacial Embedding of Laser-Manufactured Fluorinated Gold Clusters Enabling Stable Perovskite Solar Cells with Efficiency Over 24 %. Advanced materials *33*, 2101590. 10.1002/adma.202101590.
24. Xie, L., Zhang, T., Chen, L., Guo, N., and Wang, Y. (2016). Organic – inorganic interactions of single crystalline organolead halide perovskites studied by Raman spectroscopy †. Physical Chemistry Chemical Physics *18*, 18112–18118. 10.1039/C6CP01723A.
25. Hao, Y., Wang, X., Zhu, M., Jiang, X., Wang, L., Cao, G., Pang, S., and Zhou, Z. (2022). Sulfonyl passivation through synergistic hydrogen bonding and coordination interactions for efficient and stable perovskite solar cells. J Mater Chem A Mater *10*, 13048–13054. 10.1039/d2ta02084j.
26. Zhang, J., Chen, P., Yuan, B., and Ji, W. (2013). Real-Space Identification of Intermolecular Bonding with Atomic Force Microscopy. Science *342*, 611–614.
27. Wilks, R.G., Erbing, A., Sadoughi, G., Starr, D.E., Handick, E., Meyer, F., Benkert, A., Iannuzzi, M., Hauschild, D., Yang, W., Blum, M., Weinhardt, L., Heske, C., Snaith, H., Odelius, M., and Bär, M., (2021). Dynamic Effects and Hydrogen Bonding in Mixed-Halide Perovskite Solar Cell Absorbers. J Phys Chem Lett *12*, 3885–3890. 10.1021/acs.jpclett.1c00745.
28. Green, M.A., Ho-Baillie, A., and Snaith, H.J. (2014). The emergence of perovskite solar cells. Nat Photonics *8*, 506–514. 10.1038/nphoton.2014.134.
29. Kim, H.-S., Im, S.H., and Park, N.-G. (2014). Organolead Halide Perovskite: New Horizons in Solar Cell Research. The Journal of Physical Chemistry C *118*, 5615–5625.
30. Zhu, M., Li, C., Li, B., Zhang, J., and Sun, Y. (2020). Materials Horizons Interaction engineering in organic – inorganic hybrid perovskite solar cells. Mater Horiz *7*, 2208–2236. 10.1039/d0mh00745e.
31. Varadwaj, P.R., and Varadwaj, A. (2019). Significance of hydrogen bonding and other noncovalent interactions in determining octahedral tilting in the $CH_3NH_3PbI_3$ hybrid organic- inorganic halide perovskite solar cell semiconductor. Sci Rep *9*, 50. 10.1038/s41598-018-36218-1.
32. Lee, J.H., Lee, J., Kong, E., and Jang, H.M. (2016). The nature of hydrogen-bonding interaction in the prototypic hybrid halide perovskite, tetragonal. Sci Rep *6*, 21687. 10.1038/srep21687.

33. Simenas, M., Balciunas, S., Maczka, M., and Banys, J., (2022). Phase transition model of FA cation ordering in $FAPbX_3$ (X = Br, I) hybrid perovskites. J Mater Chem C Mater *10*, 5210–5217. 10.1039/d2tc00559j.
34. Pbbr, C., Mozur, E.M., Trowbridge, J.C., Maughan, A.E., Gorman, M.J., Brown, C.M., Prisk, T.R., and Neilson, J.R. (2019). Dynamical Phase Transitions and Cation Orientation-Dependent Photoconductivity in $CH(NH_2)_2PbBr_3$. ACS materilas letters *1*, 260–264. 10.1021/acsmaterialslett.9b00209.
35. Li, X., Ho, J.M., and Kanatzidis, M.G. (2021). The 2D Halide Perovskite Rulebook : How the Spacer Influences Everything from the Structure to Optoelectronic Device Efficiency. Chem Rev *121*, 2230–2291. 10.1021/acs.chemrev.0c01006.
36. Gong, J., Hao, M., Zhang, Y., Liu, M., and Zhou, Y. (2022). Layered 2D Halide Perovskites beyond the Ruddlesden – Popper Phase : Tailored Interlayer Chemistries for High- Performance Solar Cells Angewandte Minireviews. Angewandte Chemie *61*, e202112022. 10.1002/anie.202112022.
37. Li, P., Yan, L., Cao, Q., Liang, C., Zhu, H., Peng, S., Yang, Y., Liang, Y., Zhao, R., Zang, S., et al. (2023). Dredging the Charge-Carrier Transfer Pathway for Efficient Low-Dimensional Ruddlesden-Popper Perovskite Solar Cells. Angewandte Chemie International Edition *62*, e202217910. 10.1002/anie.202217910.
38. Shao, Y., Gao, W., Yan, H., Li, R., Abdelwahab, I., Chi, X., Rogée, L., Zhuang, L., Fu, W., Lau, S.P., et al. (2022). Unlocking surface octahedral tilt in two-dimensional Ruddlesden-Popper perovskites. Nat Commun *13*, 138. 10.1038/s41467-021-27747-x.
39. Ahmad, S., Fu, P., Ahmad, S., Fu, P., Yu, S., Yang, Q., Liu, X., Wang, X., and Wang, X. (2018). Dion-Jacobson Phase 2D Layered Perovskites for Solar Cells with Ultrahigh Stability Dion-Jacobson Phase 2D Layered Perovskites for Solar Cells with Ultrahigh Stability. Joule *3*, 794–806. 10.1016/j.joule.2018.11.026.
40. Lu, D., Lv, G., Xu, Z., Dong, Y., Ji, X., and Liu, Y. (2020). Thiophene-Based Two-Dimensional Dion-Jacobson Perovskite Solar Cells with over 15% Efficiency. J Am Chem Soc *142*, 11114–11122. 10.1021/jacs.0c03363.
41. Myae, C., Soe, M., Stoumpos, C.C., Kepenekian, M., Traore, B., Tsai, H., Nie, W., Wang, B., Katan, C., Seshadri, R., et al. (2017). New Type of 2D Perovskites with Alternating Cations in the Interlayer Space, $(C(NH_2)_3)(CH_3NH_3)$. J Am Chem Soc *139*, 16297–16309. 10.1021/jacs.7b09096.
42. Tsai, H., Nie, W., Blancon, J.C., Stoumpos, C.C., Asadpour, R., Harutyunyan, B., Neukirch, A.J., Verduzco, R., Crochet, J.J., Tretiak, S., et al. (2016). High-

efficiency two-dimensional ruddlesden-popper perovskite solar cells. Nature *536*, 312–317. 10.1038/nature18306.

43. Mao, L., Stoumpos, C.C., and Kanatzidis, M.G. (2019). Two-Dimensional Hybrid Halide Perovskites: Principles and Promises. J Am Chem Soc *141*, 1171–1190. 10.1021/jacs.8b10851.
44. Films, P., Cheng, L., Liu, Z., Li, S., Zhai, Y., Wang, X., Qiao, Z., Xu, Q., Meng, K., Zhu, Z., et al. (2021). Highly Thermostable and Efficient Formamidinium-Based Low-Dimensional Perovskite Solar Cells Research Articles. Angewandte Chemie *60*, 856–864. 10.1002/anie.202006970.
45. Zhu, T., Shen, L., Xun, S., Sarmiento, J.S., Yang, Y., Zheng, L., Li, H., Wang, H., Bredas, J.L., and Gong, X. (2022). High-Performance Ternary Perovskite–Organic Solar Cells. Advanced Materials *34*, 2109348. 10.1002/adma.202109348.
46. Liu, Y., Gao, S., Chen, C., Wu, Z., Gao, P., Chen, X., and Qin, T. (2022). Regulating the Intermolecular Hydrogen Bond to Realize Directional Dimension Reduction of Lead Iodide Perovskite toward Low-Dimensional Photovoltaics. Langmuir *38*, 7225–7233. 10.1021/acs.langmuir.2c00692.
47. Li, J., Yan, K., Chen, J., Zhang, Y., Yang, W., Lian, X., Wu, G., and Chen, H. (2019). Hydrogen bond enables highly efficient and stable two-dimensional perovskite solar cells based on 4-pyridine-ethylamine. Org Electron *67*, 122–127. 10.1016/j.orgel.2019.01.017.
48. Ahmad, S., and Guo, X. (2018). Rapid development in two-dimensional layered perovskite materials and their application in solar cells. Chinese Chemical Letters *29*, 657–663. 10.1016/j.cclet.2017.08.057.
49. Grancini, G., Roldán-Carmona, C., Zimmermann, I., Mosconi, E., Lee, X., Martineau, D., Narbey, S., Oswald, F., De Angelis, F., Graetzel, M., et al. (2017). One-Year stable perovskite solar cells by 2D/3D interface engineering. Nat Commun *8*, 15684.
50. Azmi, R., Ugur, E., Seitkhan, A., Aljamaan, F., Subbiah, A.S., Liu, J., Harrison, G.T., Nugraha, M.I., Eswaran, M.K., Babics, M., et al. (2022). Damp heat – stable perovskite solar cells with tailored-dimensionality 2D / 3D heterojunctions - Supplementary Materials. Science *376*, 73–77.
51. Tosado, G.A., Zheng, E., and Yu, Q. (2020). Tuning cesium-guanidinium in formamidinium tin triiodide perovskites with an ethylenediammonium additive for efficient and stable lead-free perovskite solar cells. Mater Adv *1*, 3507–3517. 10.1039/d0ma00520g.

52. Jodlowski, A.D., Roldán-carmona, C., Grancini, G., Salado, M., Ralaiarisoa, M., Ahmad, S., Koch, N., Camacho, L., and Miguel, G. De (2017). Large guanidinium cation mixed with methylammonium in lead iodide perovskites for 19 % efficient solar cells. Nat Energy *2*, 972–979. 10.1038/s41560-017-0054-3.
53. Gao, W., Chen, C., Ran, C., Zheng, H., Dong, H., Xia, Y., Chen, Y., and Huang, W. (2020). A-Site Cation Engineering of Metal Halide Perovskites : Version 3.0 of Efficient Tin-Based Lead-Free Perovskite Solar Cells. Adv Energy Mater *30*, 2000794. 10.1002/adfm.202000794.
54. Tai, Q., Cao, J., Wang, T., and Yan, F. (2019). Recent advances toward efficient and stable tin-based perovskite solar cells. EcoMat *1*, 1–15. 10.1002/eom2.12004.
55. Dey, K., Roose, B., and Stranks, S.D. (2021). Optoelectronic Properties of Low-Bandgap Halide Perovskites for Solar Cell Applications. Advanced Materials *33*, 2102300. 10.1002/adma.202102300.
56. Chowdhury, T.H., Kaneko, R., Kaneko, T., and Sodeyama, K. (2022). Electronic defect passivation of $FASnI_3$ films by simultaneous Hydrogen-bonding and chlorine co-ordination for highly efficient and stable perovskite solar cells. Chemical Engineering Journal *431*, 133745. 10.1016/j.cej.2021.133745.
57. Rao, L., Meng, X., Xiao, S., Xing, Z., Fu, Q., Wang, H., Gong, C., Hu, T., Hu, X., Guo, R., et al. (2021). Wearable Tin-Based Perovskite Solar Cells Achieved by a Crystallographic Size Effect. Angewandte Chemie *133*, 14814–14821. 10.1002/ange.202104201.
58. Amat, A., Mosconi, E., Ronca, E., Quarti, C., Umari, P., Nazeeruddin, K., Gra, M., and Angelis, F. De (2014). Cation-Induced Band-Gap Tuning in Organohalide Perovskites: Interplay of Spin − Orbit Coupling and Octahedra Tilting. Nano Lett *14*, 3608–3616.
59. Zhang, F., Park, S.Y., Yao, C., Lu, H., Dunfield, S.P., Xiao, C., Uličná, S., Zhao, X., Hill, L. Du, Chen, X., et al. (2022). Metastable Dion-Jacobson 2D structure enables efficient and stable perovskite solar cells. Science *375*, 71–76. 10.1126/science.abj2637.
60. Sun, S., Isikgor, F.H., Deng, Z., Wei, F., Kieslich, G., Bristowe, P.D., Ouyang, J., and Cheetham, A.K. (2017). Factors Influencing the Mechanical Properties of Formamidinium Lead Halides and Related Hybrid Perovskites. ChemSusChem *10*, 3740–3745. 10.1002/cssc.201700991.
61. Weller, M.T., Weber, O.J., Henry, P.F., Pumpo, M. Di, and Hansen, T.C. (2015). Complete structure and cation orientation in the perovskite photovoltaic

methylammonium lead iodide between 100 and 352 K †. Chemical Communications *51*, 4180–4183. 10.1039/c4cc09944c.

62. Butler, K.T., Svane, K., Kieslich, G., Cheetham, A.K., and Walsh, A. (2016). Microscopic origin of entropy-driven polymorphism in hybrid organic-inorganic perovskite materials. Phys Rev B *94*, 180103. 10.1103/PhysRevB.94.180103.
63. She, L., Liu, M., and Zhong, D. (2016). Atomic structures of CH3NH3PbI3 (001) surfaces. ACS Nano *10*, 1126–1131. 10.1021/acsnano.5b06420.
64. Nan, G., Beljonne, D., Zhang, X., and Quarti, C. (2020). Organic Cations Protect Methylammonium Lead Iodide Perovskites against Small Exciton-Polaron Formation. Journal of Physical Chemistry Letters *11*, 2983–2991. 10.1021/acs.jpclett.0c00673.
65. Zhang, C., Tang, Q., Zhang, M., and Nan, G. (2022). Iodide and charge migration at defective surfaces of methylammonium lead triiodide perovskites: The role of hydrogen bonding. Appl Surf Sci *604*. 10.1016/j.apsusc.2022.154501.
66. Lee, J.H., Bristowe, N.C., Bristowe, P.D., and Cheetham, A.K. (2015). Role of hydrogen-bonding and its interplay with octahedral tilting in CH3NH3PbI3. Chemical Communications *51*, 6434–6437. 10.1039/c5cc00979k.
67. Jones, T.W., Osherov, A., Alsari, M., Sponseller, M., Duck, B.C., Jung, Y.K., Settens, C., Niroui, F., Brenes, R., Stan, C. V., et al. (2019). Lattice strain causes non-radiative losses in halide perovskites. Energy Environ Sci *12*, 596–606. 10.1039/c8ee02751j.
68. Ghosh, D., Walsh Atkins, P., Islam, M.S., Walker, A.B., and Eames, C. (2017). Good Vibrations: Locking of Octahedral Tilting in Mixed-Cation Iodide Perovskites for Solar Cells. ACS Energy Lett *2*, 2424–2429. 10.1021/acsenergylett.7b00729.
69. Ghosh, D., Smith, A.R., Walker, A.B., and Islam, M.S. (2018). Mixed A-Cation Perovskites for Solar Cells: Atomic-Scale Insights into Structural Distortion, Hydrogen Bonding, and Electronic Properties. Chemistry of Materials *30*, 5194–5204. 10.1021/acs.chemmater.8b01851.
70. Lee, J., and Park, N. (2019). Chemical Approaches for Stabilizing Perovskite Solar Cells. Adv Energy Mater *10*, 1903249. 10.1002/aenm.201903249.
71. Turren-Cruz, S.H., Hagfeldt, A., and Saliba, M. (2018). Methylammonium-free, high-performance, and stable perovskite solar cells on a planar architecture. Science *362*, 449–453. 10.1126/science.aat3583.

72. Wang, S., Jiang, Y., Juarez-Perez, E.J., Ono, L.K., and Qi, Y. (2016). Accelerated degradation of methylammonium lead iodide perovskites induced by exposure to iodine vapour. Nat Energy *2*, 16195. 10.1038/nenergy.2016.195.
73. Li, X., Ke, S., Feng, X., Zhao, X., Zhang, W., and Fang, J. (2021). Enhancing the stability of perovskite solar cells through cross-linkable and hydrogen bonding. J Mater Chem A Mater *9*, 12684–12689. 10.1039/d1ta01572a.
74. Zhao, Y., Wei, J., Li, H., Yan, Y., Zhou, W., Yu, D., and Zhao, Q. (2016). A polymer scaffold for self-healing perovskite solar cells. Nat Commun *7*, 10228. 10.1038/ncomms10228.
75. Yang, J., Liu, C., Cai, C., Hu, X., Huang, Z., Duan, X., Meng, X., Yuan, Z., Tan, L., and Chen, Y. (2019). High-Performance Perovskite Solar Cells with Excellent Humidity and Thermo-Stability via Fluorinated Perylenediimide. Adv Energy Mater *9*, 1–9. 10.1002/aenm.201900198.
76. Cave, J.M., Courtier, N.E., Blakborn, I.A., Jones, T.W., Ghosh, D., Anderson, K.F., Lin, L., Dijkhoff, A.A., Wilson, G.J., Feron, K., et al. (2020). Deducing transport properties of mobile vacancies from perovskite solar cell characteristics. J Appl Phys *128*, 184501. 10.1063/5.0021849.
77. Wang, K., Zheng, L., Zhu, T., Liu, L., Becker, M.L., and Gong, X. (2020). High performance perovskites solar cells by hybrid perovskites co-crystallized with poly(ethylene oxide). Nano Energy *67*, 104229. 10.1016/j.nanoen.2019.104229.
78. Gu, X., Xiang, W., Tian, Q., and Liu, S. (Frank) (2021). Rational Surface-Defect Control via Designed Passivation for High-Efficiency Inorganic Perovskite Solar Cells. Angewandte Chemie *133*, 23348–23354. 10.1002/ange.202109724.
79. Hsu, H., Hsiao, H., Juang, T., Jiang, B., Chen, S., Jeng, R., and Chen, C. (2018). Carbon Nanodot Additives Realize High-Performance Air- Stable p–i–n Perovskite Solar Cells Providing Efficiencies of up to 20.2 %. Adv Energy Mater *8*, 1802323. 10.1002/aenm.201802323.
80. Lin, L., Jones, T.W., Yang, T.C., Duffy, N.W., Li, J., Zhao, L., Chi, B., Wang, X., and Wilson, G.J. (2021). Inorganic Electron Transport Materials in Perovskite Solar Cells. Adv Funct Mater *31*, 2008300. 10.1002/adfm.202008300.
81. Lian, J., Lu, B., Niu, F., Zeng, P., and Zhan, X. (2018). Electron-Transport Materials in Perovskite Solar Cells. Small Methods *2*, 1800082. 10.1002/smtd.201800082.
82. Bai, Y., Dong, Q., Shao, Y., Deng, Y., Wang, Q., Shen, L., Wang, D., Wei, W., and Huang, J. (2016). Enhancing stability and efficiency of perovskite solar cells with

crosslinkable silane-functionalized and doped fullerene. Nat Commun *7*, 12806. 10.1038/ncomms12806.

83. Wei, J., Guo, F., Wang, X., Xu, K., Lei, M., Liang, Y., Zhao, Y., and Xu, D. (2018). SnO_2-in-Polymer Matrix for High-Efficiency Perovskite Solar Cells with Improved Reproducibility and Stability. Advanced Materials *30*, 1805153. 10.1002/adma.201805153.
84. Huang, H., and Cui, P. (2022). 24.8%-efficient planar perovskite solar cells via ligand-engineered TiO2 deposition. Joule *6*, 1–17. 10.1016/j.joule.2022.07.004.
85. Javier Urieta-Mora, Inés García-Benito, A.M.-O. and N.M. (2018). Hole transporting materials for perovskite solar cells: a chemical approach Javier. Chem Soc Rev *47*, 8541–8571. 10.1039/c8cs00262b.
86. Pham, H.D., Yang, T.C., Jain, S.M., and Wilson, G.J. (2020). Development of Dopant-Free Organic Hole Transporting Materials for Perovskite Solar Cells. Adv Energy Mater *10*, 1903326. 10.1002/aenm.201903326.
87. Zhang, H., Liu, K., Wu, K.-Y., Chen, Y.-M., Deng, R., Li, X., Jin, H., Li, S., Chuang, S.S.C., Wang, C.-L., et al. (2018). Hydrogen-Bonding-Mediated Solid-State Self-Assembled Isoepindolidiones (isoEpi) Crystal for Organic Field-Effect Transistor. The Journal of Physical Chemistry C *122*, 5888–5895. 10.1021/acs.jpcc.7b11992.
88. Wang, C., Liu, M., Rahman, S., Pekka, H., Tian, J., Li, J., Deng, Z., Zhang, H., and Vivo, P. (2022). Hydrogen bonding drives the self-assembling of carbazole-based hole-transport material for enhanced efficiency and stability of perovskite solar cells. Nano Energy *101*, 107604. 10.1016/j.nanoen.2022.107604.
89. Kaneko, R., Chowdhury, T.H., Sugawa, K., Lee, J.J., Otsuki, J., and Islam, A. (2019). Electro-active nanofibers of a tetrathiafulvalene derivative with amide hydrogen bonds as a dopant-free hole transport material for perovskite solar cells. Solar Energy *194*, 248–253. 10.1016/j.solener.2019.10.078.
90. Li, R., Li, C., Liu, M., Vivo, P., Zheng, M., Dai, Z., Zhan, J., He, B., Li, H., Yang, W., et al. (2021). Hydrogen-Bonded Dopant-Free Hole Transport Material Enables Efficient and Stable Inverted Perovskite Solar Cells. CCS Chemistry *3*, 3309–3319. 10.31635/ccschem.021.202101483.
91. Wang, S., Li, Y., Yang, J., Wang, T., Yang, B., Cao, Q., Pu, X., Etgar, L., Han, J., Zhao, J., et al. (2022). Critical Role of Removing Impurities in Nickel Oxide on High-Efficiency and Long-Term Stability of Inverted Perovskite Solar Cells. Angewandte Chemie International Edition *61*, e202116534. https://doi.org/10.1002/anie.202116534.

92. Peng, J., Wu, Y., Wang, Y., Jacobs, D., Shen, H., Fu, X., Wan, Y., Duong, T., Wu, N., Barugkin, C., et al. (2017). Interface passivation using ultrathin polymer-fullerene films for high-efficiency perovskite solar cells with negligible hysteresis. Energy Environ. Sci. *10*, 1792–1800. 10.1039/C7EE01096F.
93. Wang, M., Zhao, Y., Jiang, X., Jin, S., Wang, M., Zhao, Y., Jiang, X., Yin, Y., Yavuz, I., and Zhu, P. (2022). Rational selection of the polymeric structure for interface engineering of perovskite solar cells structure for interface engineering. Joule *6*, 1032–1048. 10.1016/j.joule.2022.04.002.
94. Wolff, C.M., Caprioglio, P., Stolterfoht, M., and Neher, D. (2019). Nonradiative Recombination in Perovskite Solar Cells : The Role of Interfaces. Adv Energy Mater *31*, 1902762. 10.1002/adma.201902762.
95. Zheng, L., Mukherjee, S., Wang, K., Hay, M.E., Boudouris, B.W., and Gong, X. (2017). Radical polymers as interfacial layers in inverted hybrid perovskite solar cells. J Mater Chem A Mater *5*, 23831–23839. 10.1039/c7ta07732g.
96. Wang, S., Li, Y., Yang, J., Wang, T., Yang, B., Cao, Q., and Pu, X. (2022). Critical Role of Removing Impurities in Nickel Oxide on High- Efficiency and Long-Term Stability of Inverted Perovskite Solar Cells. Angewandte Chemie *61*, e202116534. 10.1002/anie.202116534.
97. Sin, D.H., Jo, S.B., Lee, S.G., Ko, H., Kim, M., Lee, H., and Cho, K. (2017). Enhancing the Durability and Carrier Selectivity of Perovskite Solar Cells Using a Blend Interlayer. ACS Appl Mater Interfaces *9*, 18103–18112. 10.1021/acsami.7b02349.
98. Li, N., Tao, S., Chen, Y., Niu, X., Onwudinanti, C.K., Hu, C., Qiu, Z., Xu, Z., Zheng, G., Wang, L., et al. (2019). Cation and anion immobilization through chemical bonding enhancement with fluorides for stable halide perovskite solar cells. Nat Energy *4*, 408–415. 10.1038/s41560-019-0382-6.
99. Liu, J., De Bastiani, M., Aydin, E., Harrison, G.T., Gao, Y., Pradhan, R.R., Eswaran, M.K., Mandal, M., Yan, W., Seitkhan, A., et al. (2022). Efficient and stable perovskite-silicon tandem solar cells through contact displacement by MgFx. Science *377*, 302–306. 10.1126/science.abn8910.
100. Bai, S., Da, P., Li, C., Wang, Z., Yuan, Z., Fu, F., Kawecki, M., Liu, X., Sakai, N., Wang, J.T.W., et al. (2019). Planar perovskite solar cells with long-term stability using ionic liquid additives. Nature *571*, 245–250. 10.1038/s41586-019-1357-2.
101. Lin, Y., Sakai, N., Da, P., Wu, J., Sansom, H.C., Ramadan, A.J., Sharma, K., Madhu, P.K., Vilches, A.B.M., Nayak, P.K., et al. (2020). A piperidinium salt stabilizes efficient metal-halide perovskite solar cells. Science *369*, 96–102.

102. Giron, R.G.P., and Ferguson, G.S. (2017). Tetrafluoroborate and Hexafluorophosphate Ions are not Interchangeable: A Density Functional Theory Comparison of Hydrogen Bonding. ChemistrySelect *2*, 10895–10901. https://doi.org/10.1002/slct.201702176.
103. Chen, X., Zhang, X., Liu, D., Huang, R., Wang, S., Xiong, L., Zhang, W., and Chen, X. (2021). Room-temperature ferroelectric and ferroelastic orders coexisting in a new tetrafluoroborate-based perovskite. Chem Sci *12*, 8713–8721. 10.1039/d1sc01345a.
104. Nagane, S., Macpherson, S., Hope, M.A., Kubicki, D.J., Li, W., Verma, S.D., Ferrer Orri, J., Chiang, Y.H., MacManus-Driscoll, J.L., Grey, C.P., et al. (2021). Tetrafluoroborate-Induced Reduction in Defect Density in Hybrid Perovskites through Halide Management. Advanced Materials *33*, 2102462. 10.1002/adma.202102462.
105. Gillespie, R.J., Hartman, J.S., and Parekh, M. (1968). Solvent effects on the boron-fluorine coupling constant and on fluorine exchange in the tetrafluoroborate anion. Can J Chem *46*, 1601. 10.1139/v68-268.
106. Zheng, X., Chen, B., Dai, J., Fang, Y., Bai, Y., Lin, Y., Wei, H., Zeng, X.C., and Huang, J. (2017). Defect passivation in hybrid perovskite solar cells using quaternary ammonium halide anions and cations. Nat Energy *2*, 17102. 10.1038/nenergy.2017.102.
107. Abbott, A.P., Capper, G., Davies, D.L., Rasheed, R.K., and Tambyrajah, V. (2003). Novel solvent properties of choline chloride/urea mixtures. Chemical Communications, 70–71. 10.1039/b210714g.
108. Stefanovic, R., Ludwig, M., Webber, G.B., Atkin, R., and Page, A.J. (2017). Nanostructure, hydrogen bonding and rheology in choline chloride deep eutectic solvents as a function of the hydrogen bond donor. Physical Chemistry Chemical Physics *19*, 3297–3306. 10.1039/c6cp07932f.
109. Ghosh, D., Smith, A.R., Walker, A.B., and Islam, M.S. (2018). Mixed A - Cation Perovskites for Solar Cells: Atomic-Scale Insights Into Structural Distortion, Hydrogen Bonding, and Electronic Properties. Chemistry of Materials *30*, 5194–5204. 10.1021/acs.chemmater.8b01851.
110. Cornell, W.D., Cieplak, P., Bayly, C.I., Gould, I.R., Merz, K.M., Ferguson, D.M., Spellmeyer, D.C., Fox, T., Caldwell, J.W., and Kollman, P.A. (1995). A Second Generation Force Field for the Simulation of Proteins, Nucleic Acids, and Organic Molecules. J Am Chem Soc *117*, 5179–5197. 10.1021/ja00124a002.

111. Li, X.Z., Walker, B., and Michaelides, A. (2011). Quantum nature of the hydrogen bond. Proc Natl Acad Sci U S A *108*, 6369–6373. 10.1073/pnas.1016653108.
112. Mata, I., Alkorta, I., Espinosa, E., and Molins, E. (2011). Relationships between interaction energy, intermolecular distance and electron density properties in hydrogen bonded complexes under external electric fields. Chem Phys Lett *507*, 185–189. 10.1016/j.cplett.2011.03.055.
113. Sun, J., Ruzsinszky, A., and Perdew, J. (2015). Strongly Constrained and Appropriately Normed Semilocal Density Functional. Phys Rev Lett *115*, 036402. 10.1103/PhysRevLett.115.036402.
114. Oranskaia, A., Yin, J., Bakr, O.M., Brédas, J.L., and Mohammed, O.F. (2018). Halogen Migration in Hybrid Perovskites: The Organic Cation Matters. Journal of Physical Chemistry Letters *9*, 5474–5480. 10.1021/acs.jpclett.8b02522.
115. Zhu, Z., Hadjiev, V.G., Rong, Y., Guo, R., Cao, B., Tang, Z., Qin, F., Guloy, A.M., Fang, H., Hu, Y., et al. (2016). Interaction of Organic Cation with Water Molecule in Perovskite $MAPbI_3$: From Dynamic Orientational Disorder to Hydrogen Bonding. Chemistry of Materials *28*, 7385–7393. 10.1021/acs.chemmater.6b02883.
116. Christians, J.A., Miranda Herrera, P.A., and Kamat, P. V. (2015). Transformation of the excited state and photovoltaic efficiency of $CH_3NH_3PbI_3$ perovskite upon controlled exposure to humidified air. J Am Chem Soc *137*, 1530–1538. 10.1021/ja511132a.
117. Leguy, A.M.A., Hu, Y., Campoy-Quiles, M., Alonso, M.I., Weber, O.J., Azarhoosh, P., Van Schilfgaarde, M., Weller, M.T., Bein, T., Nelson, J., et al. (2015). Reversible hydration of $CH_3NH_3PbI_3$ in films, single crystals, and solar cells. Chemistry of Materials *27*, 3397–3407. 10.1021/acs.chemmater.5b00660.
118. Yang, J., Siempelkamp, B.D., Liu, D., and Kelly, T.L. (2015). Investigation of $CH_3NH_3PbI_3$ Degradation Rates and Mechanisms in Controlled Humidity Environments Using in Situ Techniques. ACS Nano *9*, 1955–1963. 10.1021/nn506864k.
119. Zhang, L., and Sit, P.H.L. (2015). Ab Initio Study of Interaction of Water, Hydroxyl Radicals, and Hydroxide Ions with $CH_3NH_3PbI_3$ and $CH_3NH_3PbBr_3$ Surfaces. Journal of Physical Chemistry C *119*, 22370–22378. 10.1021/acs.jpcc.5b07000.
120. Song, Z., Abate, A., Watthage, S.C., Liyanage, G.K., Phillips, A.B., Steiner, U., Graetzel, M., and Heben, M.J. (2016). Perovskite Solar Cell Stability in Humid Air: Partially Reversible Phase Transitions in the PbI_2-CH_3NH_3I-H_2O System. Adv Energy Mater *6*, 1600846. 10.1002/aenm.201600846.

121. Huang, J., and Lund, P.D. (2017). Environmental Science Impact of H_2O on organic–inorganic hybrid perovskite solar cells. Energy Environ Sci *10*, 2284–2311. 10.1039/c7ee01674c.
122. Gao, Y., Xu, W., He, F., Fan, T., Cai, W., Zhang, X., and Wei, G. (2022). Boosting Performance of $CsPbI_3$ Perovskite Solar Cells via the Synergy of Hydroiodic Acid and Deionized Water. advanced energy sustainability research *3*, 2100149. 10.1002/aesr.202100149.
123. Wang, F., Yang, M., Zhang, Y., Yang, L., Fan, L., and Lv, S. (2018). Activating Old Materials with New Architecture: Boosting Performance of Perovskite Solar Cells with H_2O-Assisted Hierarchical Electron Transporting Layers. Advanced Science *6*, 1801170. 10.1002/advs.201801170.
124. Zhu, J., Kim, D.H., Kim, J.D., Lee, D.G., Kim, W. Bin, Chen, S.W., Kim, J.Y., Lee, J.M., Lee, H., Han, G.S., et al. (2021). All-in-One Lewis Base for Enhanced Precursor and Device Stability in Highly Efficient Perovskite Solar Cells. ACS Energy Lett *6*, 3425–3434. 10.1021/acsenergylett.1c01465.
125. Hartono, N.T.P., Thapa, J., Tiihonen, A., Oviedo, F., Batali, C., Yoo, J.J., Liu, Z., Li, R., Marrón, D.F., Bawendi, M.G., et al. (2020). How machine learning can help select capping layers to suppress perovskite degradation. Nat Commun *11*, 4172. 10.1038/s41467-020-17945-4.
126. Rosales, B.A., Mundt, L.E., Allen, T.G., Moore, D.T., Prince, K.J., Wolden, C.A., Rumbles, G., Schelhas, L.T., and Wheeler, L.M. (2020). Reversible multicolor chromism in layered formamidinium metal halide perovskites. Nat Commun *11*, 1–12. 10.1038/s41467-020-19009-z.
127. Zhao, P., Kim, B.J., Ren, X., Lee, D.G., Bang, G.J., Jeon, J.B., Kim, W. Bin, and Jung, H.S. (2018). Antisolvent with an Ultrawide Processing Window for the One-Step Fabrication of Efficient and Large-Area Perovskite Solar Cells. Advanced Materials *30*, 1–8. 10.1002/adma.201802763.
128. Stranks, S.D., and Plochocka, P. (2018). The influence of the Rashba effect. Nat Mater *17*, 381–382. 10.1038/s41563-018-0067-8.
129. Frohna, K., Deshpande, T., Harter, J., Peng, W., Barker, B.A., Neaton, J.B., Louie, S.G., Bakr, O.M., Hsieh, D., and Bernardi, M. (2018). Inversion symmetry and bulk Rashba effect in methylammonium lead iodide perovskite single crystals. Nat Commun *9*, 1829. 10.1038/s41467-018-04212-w.
130. Zheng, F., Tan, L.Z., Liu, S., and Rappe, A.M. (2015). Rashba Spin–Orbit Coupling Enhanced Carrier Lifetime in CH3NH3PbI3. Nano Lett *15*, 7794–7800. 10.1021/acs.nanolett.5b01854.

131. Etienne, T., Mosconi, E., and De Angelis, F. (2016). Dynamical Origin of the Rashba Effect in Organohalide Lead Perovskites: A Key to Suppressed Carrier Recombination in Perovskite Solar Cells? J Phys Chem Lett *7*, 1638–1645. 10.1021/acs.jpclett.6b00564.